University of New Hampshire
University of New Hampshire Scholars' Repository

Master's Theses and Capstones   Student Scholarship

Fall 2009

Thermal exchange processes within shallow fractured bedrock: Applications for standing column wells

Sarah B. McKone
University of New Hampshire, Durham

Follow this and additional works at: https://scholars.unh.edu/thesis

Recommended Citation

THERMAL EXCHANGE PROCESSES WITHIN SHALLOW FRACTURED

BEDROCK: APPLICATIONS FOR STANDING COLUMN WELLS

BY

Sarah B. McKone

B.S., Biology, Messiah College, 2007

THESIS

Submitted to the University of New Hampshire

In Partial Fulfillment of

The Requirements for the Degree of

Master of Science

in

Earth Sciences: Hydrology

September, 2009

UMI Number: 1472074

INFORMATION TO USERS

The quality of this reproduction is dependent upon the quality of the copy submitted. Broken or indistinct print, colored or poor quality illustrations and photographs, print bleed-through, substandard margins, and improper alignment can adversely affect reproduction.
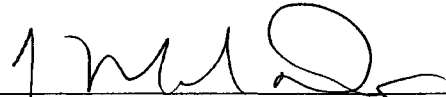
In the unlikely event that the author did not send a complete manuscript and there are missing pages, these will be noted. Also, if unauthorized copyright material had to be removed, a note will indicate the deletion.

UMI®
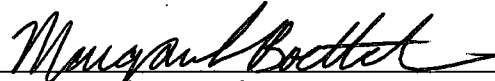
This thesis has been examined and approved.

_____

Thesis Director, J. Matthew Davis
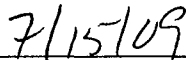Associate Professor of Hydrogeology

_____

Francis S. Birch
Professor of Earth Sciences

_____

Margaret S. Boettcher
Assistant Professor of Earth Sciences

_____

Date 7/15/09

DEDICATION

This thesis is dedicated to my younger sister Megan.

I am so proud of you,

and you continue to amaze me.

ACKNOWLEDGEMENTS

TABLE OF CONTENTS

LIST OF FIGURES

LIST OF TABLES

ABSTRACT

THERMAL EXCHANGE PROCESSES WITHIN SHALLOW FRACTURED

BEDROCK: APPLICATIONS FOR STANDING COLUMN WELLS

By

Sarah B. McKone

University of New Hampshire, September, 2009

This research investigates thermal properties of fractured bedrock for the purpose of better understanding the sustainability of standing column well (SCW) geothermal heating systems. The three objectives are to quantify effective thermal conductivity and heat capacity of the fracture network; measure heat exchange between the fluid and the fractured surfaces; and estimate time of thermal breakthrough into a pumping well. Single and dipole well tests are performed to meet these objectives. Single well data is compared with an analytical heat flow model to estimate thermal conductivity and heat capacity. Dipole well data is compared to a model of the Kolditz (1995) modification of Gringarten and Sauty's (1975) thermal breakthrough curve. Thermal conductivity is estimated to be lower than the previously reported value by Roy et al. (1968). No thermal breakthrough is observed during the dipole test, however, modeling of theoretical SCW systems shows significant temperature changes over the long term.

CHAPTER I

INTRODUCTION

Alternative heating technologies have attracted increasing attention in recent years, caused by a heightened environmental awareness in the public realm. Additionally, an impending fuel crisis resulting in a rise in oil and gas prices has led consumers to seek alternatives which may provide lower long term heating costs. Thus, alternatives providing both lower heating costs and reduced greenhouse gas emissions are very appealing. Geothermal heating systems are one of the alternative heating technologies which have recently gained significant momentum; appearing to meet the aforementioned expectations, while possibly utilizing a permanently renewable resource. However, the long term sustainability of these systems has not been thoroughly investigated.

In standard geothermal heating, cold water circulates in a closed loop in a deep bedrock well in order to be warmed. The water is then drawn up and run through a heat pump which removes the heat gained, allowing cold water to return to the well to be heated again (O'Neill et al., 2006). Ideally the warmed water is around 50 ° F before it is run through the heat pump. During seasons of warmer air temperature, geothermal systems can also be used for space cooling systems. Warm water is pumped into the well to release heat, serving both as a residential cooling system and a means to recharge the bedrock. In the northern latitudes, where heating demand exceeds cooling, use of geothermal systems year round may still result in a net heat extraction. Conversely, in

1

Southern latitudes where the cooling demand is greater, use of a geothermal system year round may result in net heat injection.

Standing Column Wells (SCW) are one variety of geothermal heating systems which utilize wells similar to, or the same as, those used for residential drinking water. Instead of a closed loop system, water is circulated through the open well, placing the water directly in contact with the bedrock. Additional water is drawn from the well in a process called bleeding, whereby water is regularly pumped out of the SCW in order to draw warmer water from distal bedrock. Thus, thermal transfer in the Standing Column Well occurs through both conductive heat flow from the surrounding bedrock, and advective flow as water is drawn into the well (Figure 1.1, adapted from Rees et al., 2004). Bleed flow increases heating efficiency by moderating the water temperature, improving the performance more dramatically than all other system parameters (Rees, 2004). As advective flow brings warm water from further horizontal and vertical distances than by conduction alone, it also reduces the necessary well depth and prevents well freeze (Rees et al., 2004). Unfortunately, bleeding causes many hundreds of gallons to be diverted from the well, and after heat extraction the water is typically discharged to the surface where it either re-infiltrates or runs off. Subsequently, the well's aquifer has a high water output demand (Rees et al., 2004).

Dipole well arrangements are sometimes utilized in SCW systems, whereby warm water is withdrawn from one well, and injected into a second well as cold water after being run through a heat exchanger (Ferguson, 2006). Spatial limitation of most residential arrangements has occasionally led to breakthrough of cool water into the heating well or gradual temperature drop leading to inefficient or unstable systems

2

(Kocabas, 2005). Considering the heat output a given fracture network is required to produce, heat conduction to the fractures may not be sufficient to maintain necessary water temperatures over the long term. Because the uptake of heat within fractures is more easily quantified than the release of heat from the bedrock, this research will utilize heat injection in order to analyze thermal properties. However, the discussion on sustainability will focus on wintertime heat extraction from wells, with the knowledge that the system can be reversed during cooling mode.

Previous Studies

Kocobas (2005) proposes a testing procedure for quantifying the thermal properties of an aquifer utilizing slug injection of a tracer, followed by injection of low temperature water, while monitoring for the fronts of both injections in a pumping well. A similar method of field testing is used for this thesis; however, the use of warm injection water is one modification upon the Kocobas (2005) method. Concerning thermal breakthrough, there exist a set of solutions for calculating heat loss in a pumping well caused by the presence of water with a lower temperature than that of the ambient water in the aquifer. The source may be a reinjection well in a dipole well set, or an aquifer recharge area. Gringarten and Sauty (1975) develop an analytical solution for application to a horizontal aquifer of known thickness and steady and uniform regional flow (Gringarten and Sauty, 1975). For the purposes of this study the fracture aperture will be used as a substitute for the aquifer of known thickness, therefore, the Kolditz (2006) modification of the Gringarten and Sauty (1975) solution is most appropriate. Additionally, Gringarten and Sauty (1975) model a dipole system with equal rates of injection and withdrawal. The system in this investigation maintains a constant pumping

rate, but has a limited injection pressure which is unable to achieve input rates equal to those of the output, and therefore will experience temperature breakthrough at a delayed rate compared to that of the model.

Project Overview

The purpose of this thesis is to characterize the heat exchange properties of fractured bedrock in order to quantify the long term sustainability of standing column wells (SCWs) as alternative heating/cooling systems. Two varieties of field tests were performed on five different shallow fractured bedrock wells representative of those used for residential geothermal heating units in the Northeastern United States. Additionally, model temperature scenarios were calculated based on known and modeled parameters and previous research dealing with geothermal systems.

In investigating thermal processes, this research has three objectives. First, quantify the effective thermal conductivity and heat capacity of the fracture network. Together these parameters express the amount of heat the bedrock is capable of transferring and storing (Gul, et al. 2005). Second, measure the heat exchange between the fluid, in one or more fractures, and the bedrock. Third, estimate the time of thermal breakthrough of injected water into a pumping well. Two varieties of heat injection tests are used to investigate these processes. The first, the single well test, allows the effective thermal conductivity and heat capacity in the immediate vicinity of the fractured bedrock well to be effectively modeled. The second, the dipole well test, deals with heat exchange between the fluid in one or more fractures and the bedrock, and allows thermal breakthrough times to be inferred. To date, the sustainability of SCWs as it relates to the

4

effective thermal conductivity and heat capacity of fractured bedrock has not been investigated.
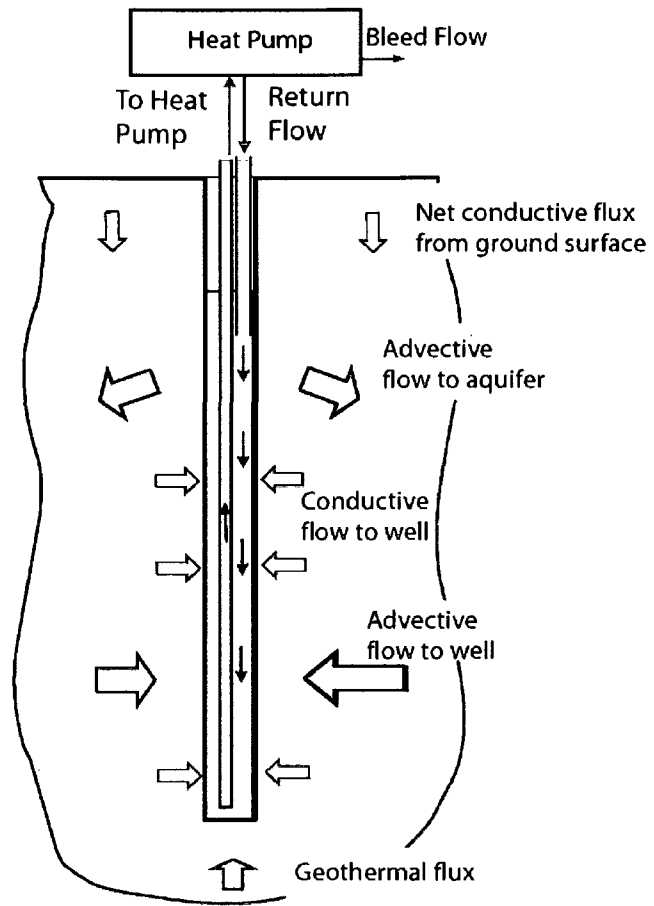
Figure 1.1 Thermal transfer in the Standing Column Well occurs through conductive heat flow, as well as advective flow as water is drawn into or leaves the open system (adapted from Rees, 2004).

CHAPTER II

FIELD METHODS

Site Description

Field testing took place at the UNH well field adjacent to the old Durham reservoir (Figure 2.1) located at 43 08'48.26"N, 70 56'32.89"W. The UNH Well Field is used primarily for teaching and research in the Department of Earth Sciences and Civil Engineering at the University of New Hampshire, and has been extensively investigated using geophysical and hydrologic methods, making it a very appropriate location for this study.

Devonian Exeter Diorite underlies the well field at about 8 meters below ground surface. Roy et al. (1968) measured the thermal conductivity of the Exeter Diorite in Durham, N.H., at 43 07'N, 70 55'W, to be 2.6 W/m°C. Glaciomarine clay deposits and sandy glacial till overlie the bedrock (Helmrath, 1999). Within the sediment, the water table lies at a depth less than 1 meter, with groundwater flow west to east. Within the bedrock, low angle fractures have been described using GPR with borehole antennae (Foster, 2000).

Nineteen wells are present on site, seven of which are deep bedrock wells. Deep bedrock wells are all approximately 46 meters in depth and are indicated by a name composed of the letter "R" followed by a number, while shallow bedrock wells are

indicated by "SR" followed by a number. Each deep bedrock well is 6-inches in diameter with steel casing set into the bedrock, and is comparable to many basic SCW systems, though not as deep. For the single well tests R2 was selected because it lacks hydraulically conductive fractures, while R3 and R4 were chosen as the hydraulically conductive testing locations based on pump tests during field work. Of the deep bedrock wells available, injection and pumping wells for the dipole well test were selected based on preliminary pump tests. Dipole well tests were performed three times, with R3 serving as the pumping well each time, and R4, SR3 and R6 each serving as the injection well, as shown in Figure 2.2.

Thermistor Cable

In order to measure temperatures for the length of the borehole during each well test, it was necessary to construct custom apparatus. Thermistors were arranged at five foot intervals for 150 feet, each attached to a circuit converting the temperature-dependant resistance into a voltage. The voltage for each thermistor was collected by a battery powered Campbell Scientific CR1000 datalogger equipped with a Campbell Scientific AM16/32B, 32-channel relay multiplexer. Voltages were recorded at 5 minute intervals. Wiring diagrams for the circuit multiplexer, and datalogger are provided in Appendix A.

Lab testing of the thermistor cable was conducted by submersing the 150 ft cable in a 5-foot long water filled cylinder. This enabled evaluation of proper waterproofing of all seals and identification of outlying resistivity measurements. Temperature data was collected by Campbell Scientific 109 Temperature Probes at three locations along the tube and thermistor circuit voltage was compared to known temperatures for calibration.

At some locations, thermistors did not respond as expected to changes in temperature. The readings from those points were monitored individually throughout lab and field testing as possible sources of error. Unfortunately, the temperature in the cylinder was not uniform, and detailed calibration was not possible.

In order to maintain calibration throughout field testing, borehole temperatures were measured manually using a YSI model 3000 T-L-C meter during background data collection, single well tests, recovery, and dipole well tests. These measurements, as well as calibration comparisons can be found in Appendix B.

Background Temperatures

Before each single well test, background temperatures were collected for the length of the borehole using the 150 ft thermistor cable. During well tests in R2 and R3, background temperatures were recorded for 24 hours and were found to be very stable below the till-bedrock contact. Thus, background temperatures were subsequently measured for shorter periods of time. This information, as well as a timeline of all field work is provided in the table in Appendix C.

Heating Cable

A 120 foot heating cable with 3 watt per foot heat rating was chosen as the method of heating for the single well test. In order to increase the accuracy of calculations based on single well test data, the heat output of the cable was tested in a lab setting. The cable was submerged in water held by a Plexiglas column which was wrapped in fiberglass insulation. Temperature measurements were taken every 1 minute for 60 minutes using a YSI model 3000 T-L-C meter, and the column was stirred to prevent temperature stratification. The resulting temperature data allowed an adjusted

9

heat output of 3.34 watts per foot to be calculated. Details of this calculation are provided in Appendix B.

Single Well Test

Single well tests were run in wells R2, R3, and R4 individually for a duration of 60 hours each. The heating cable was powered by a 5600 watt gas-powered generator (Figure 2.3), refueled at ten hour intervals and turned off for 10 to 15 minute periods during refueling. Temperature decreases of up to 5 percent occurred during refueling, however, temperature data collection continued unaffected, as the data logger was battery powered.

Dipole Well Test

For each dipole well test, warm water (averaging 19.5 °C) was pumped from the old Durham reservoir into Well A while temperature was recorded and water pumped out of Well B as shown in Figure 2.4. Water was siphoned into Well A at a rate necessary to maintain a hydraulic head as high as possible (elevation of casing), while pumping from Well B occurred at a relatively constant rate of 4.08×10^{-4} m^3/s (6.47 gal/min). Rhodamine dye was added as a tracer in order to pinpoint the arrival time of the injected water. The thermistor cable was installed in the pumping well in order to detect thermal breakthrough during pumping. Wells serving as Well A (injection well) included SR3, R4 and R6; while well R3 served as Well B (pumping well) in every case. Additionally, water level and temperature changes were monitored in both injection wells and observation wells manually, and using Solinst LT F15/M5 Leveloggers. The pumping well (R3) had an average ambient water temperature of 9.9 °C prior to the dipole well tests. Average temperature difference between injected and ambient waters was 9.6 °C.

During the dipole well test the thermistor cable encountered interference of unknown origin, which caused it to record recurrent oscillations on the order of hundredths of degrees. Although these oscillations may have prevented the recognition of minute heat variation, this should not have interfered with the detection of thermal breakthrough.

Fluorometer Background

Fluorescence measurements were recorded by a Turner Designs Model 10-AU-005-CE flow through fluorometer, powered by the same 5600 watt generator. Background readings were taken before each rhodamine tracer test, in order to establish ambient fluorescence. Most background readings fell between 0.300 and 0.903 parts per billion (ppb), with the highest not exceeding 1.100 ppb. Background readings were low enough to never be mistaken for the actual rhodamine breakthrough to the pumping well.

Rhodamine Injection

Each rhodamine injection was performed as a single slug addition. In order to introduce the tracer over the entire borehole, rhodamine was injected near the bottom of the well using a funnel attached to the injection hose, and flushed out with additional water. For the dipole test between well SR4 and well R3, approximately 1000 mL of 4000 ppm rhodamine was added. For the dipole test between well R4 and well R3 approximately 300 mL of 4000 ppm rhodamine was added. For the dipole test between well R6 and well R3, 70 mL of 25000 ppm rhodamine was added.

In order to detect the arrival of rhodamine in the pumping well, the outflow hose was connected to the flow through attachment of the fluorometer, which ran continuously and logged concentration at one minute intervals. During some tests the fluorometer was

run for long spans of time, making it necessary to turn it off briefly for refueling of the generator. After each power-off the fluorometer appeared to make a full recovery to previous ppb levels; this is not assumed to be a significant source of error.

Data Analysis

Single well test heating is analyzed using a heat flow model, with a form similar to the Theis equation (Schwartz and Zhang, 2003). The result is

$$s = \frac{Q}{4\pi C} W(u)$$

where s is change in temperature, Q is pumping rate, C is thermal conductivity times b, b is the saturated thickness, and W(u) is the well function where

$$u = \frac{r^2 H}{4Ct}$$

with t being equal to time, and H equal to heat capacity times b. Each single well test is compared to the heat flow model. Observation wells SR3 and MW5 are also modeled and compared to drawdown data during pumping for the dipole well test. However, the presence of borehole storage prevents a direct comparison between the modeled and observed outcome during this test. Figures illustrating observed and modeled drawdowns for each test are provided in Appendix B. Transmissivity during pumping was calculated using drawdown data from observation wells and the Theim equation (Signorelli, 2004),

$$T = \frac{2.3Q}{2\pi(s_1 - s_2)} log_{10} \frac{r_2}{r_1} \tag{2.1}$$

where the parameter values are found in the table 2.1.

Table 2.1 Hydraulic Parameter definitions for the Theim equation

Symbol	Definition	Value
T	transmissivity of aquifer	Unit of m^2/day or m^2/sec
Q	pumping rate of well (positive for withdrawal and negative for injection)	4.08×10^{-4} m^3/s or 35.249 m^3/day
s1	Drawdown in the first well(R3)	4.85 m
s2	Drawdown in the second well (R4)	3.12 m
r1	Distance from pumping to first well (R3)	0.076 m
r2	Distance from pumping to the second well (R4)	26.21 m

Fracture aperture was calculated using a modified version of the hydraulic

conductivity equation $K = \frac{(\rho_w g b^2)}{(12\mu)}$ and the transmissivity equation, $T = Kb$ (Schwartz

and Zhang, 2003). The result is

$$b = \left(\frac{12\mu}{\rho_w g}\right)^{1/3} \tag{2.2}$$

where the parameter values are found in table 2.2.

Table 2.2 Parameter definitions for the equation 2.2, for finding fracture aperture.

Symbol	Definition	Value
T	Transmissivity	18.92 m^2/day or $2.1910^{-4} m^2$/sec
b	aquifer thickness (fracture aperture)	Unit of m
K	hydraulic conductivity	Unit of m/day or m/sec
Pw	density of water	998.2 kg/m^3
g	gravitational acceleration	9.8 m/sec^2
μ	viscosity of water (at 10 degrees)	1.308×10^{-3} kg·m^{-1}·s^{-1}

Temperature change in the pumping well during the dipole well test is

approximated using the analytical model by Gringarten and Sauty (1975) as modified by

Kolditz (1995) for a single fracture.

$$T_D = u(t_D - I_D) \; erfc\left\{ \frac{\beta \, I_D}{\sqrt{\alpha(t_D - I_D)}} \right\}, \; z_D = \frac{1}{2} \tag{2.3}$$

Where $I_D\left(\varphi(x_D, 0), (\psi(x_D, 0)) \right) =$

$\frac{2\pi}{3} \frac{a^2}{w^2} \left\{ 1 - \frac{sinh\varphi}{cosh\varphi + cos\psi} \left(1 + \frac{cos\psi}{cosh\varphi + cos\psi} \right) \right\}$, $|cos\psi| = 1$, T_D is dimensionless

temperature, and remaining parameters are found in table 2.3.

Table 2.3 Parameter definitions for the equation Kolditz (1995) equation.

Symbol	Definition	Value
x	distance between wells	32.92 meters for R4 to R3 26.21 meters for R6 to R3 60.96 meters for image well to R3
y	horizontal distance from bisect	0 meters
z	distance from center of fracture	w/2 meters
a	half borehole separation	x/2 meters
x_D	$x_D = \frac{x}{a}$	2 (unitless)
y_D	$y_D = \frac{y}{a}$	0 (unitless)
z_D	$z_D = \frac{z}{w}$	½ (unitless)
w	fracture aperture	7.06×10^{-4} m
Q	pumping rate	4.08×10^{-4} m^3/day
$c_r \rho_r$	bedrock specific heat density	2.2×10^{-6} J/m^3
$c_w \rho_w$	water specific heat density	4.186×10^{-6} J/m^3
λ_r	rock thermal conductivity	2.00 w/mC
I_D	(see above)	1.49×10^9 for R4 to R3 2.35×10^9 for R6 to R3 8.05×10^9 for image well to R3
t_D	$t_D = \frac{Q}{w^3} t$	(unitless variable)
β	$\beta = \frac{\lambda_r}{c_w \rho_w} \frac{w}{Q}$	8.27×10^{-7} (unitless)
α	$\alpha = \frac{\lambda_r}{c_r \rho_r} \frac{w}{Q}$	1.57×10^{-6} (unitless)
φ	$\varphi = \frac{1}{2} ln \frac{(x_D - 1)^2 + y_D^2}{(x_D - 1)^2 - y_D^2}$	0 (unitless)
ψ	$\psi = \arctan \frac{2y_D}{1 - (x_D^2 - y_D^2)}$	0 (unitless)
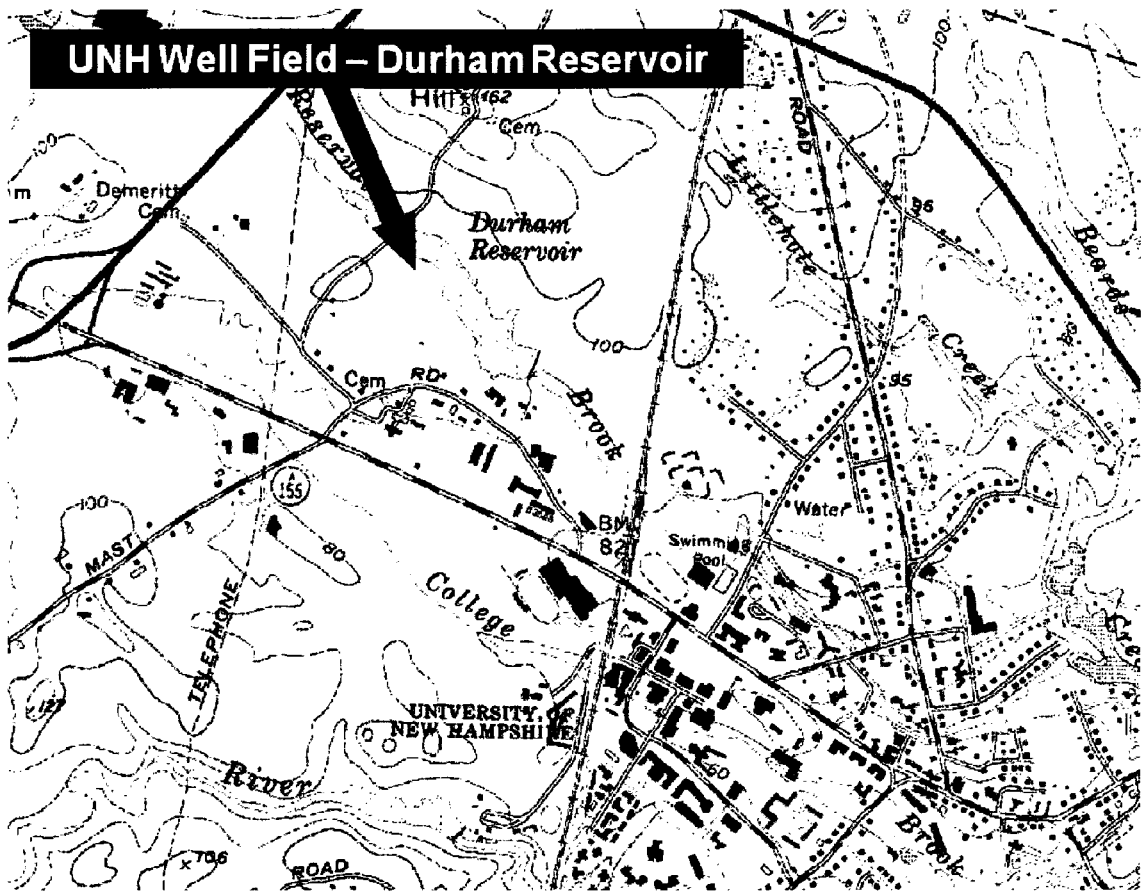
Figure 2.1 The UNH well field, beside the Durham Reservior, in relation to the main campus of the University of New Hampshire in Durham NH.
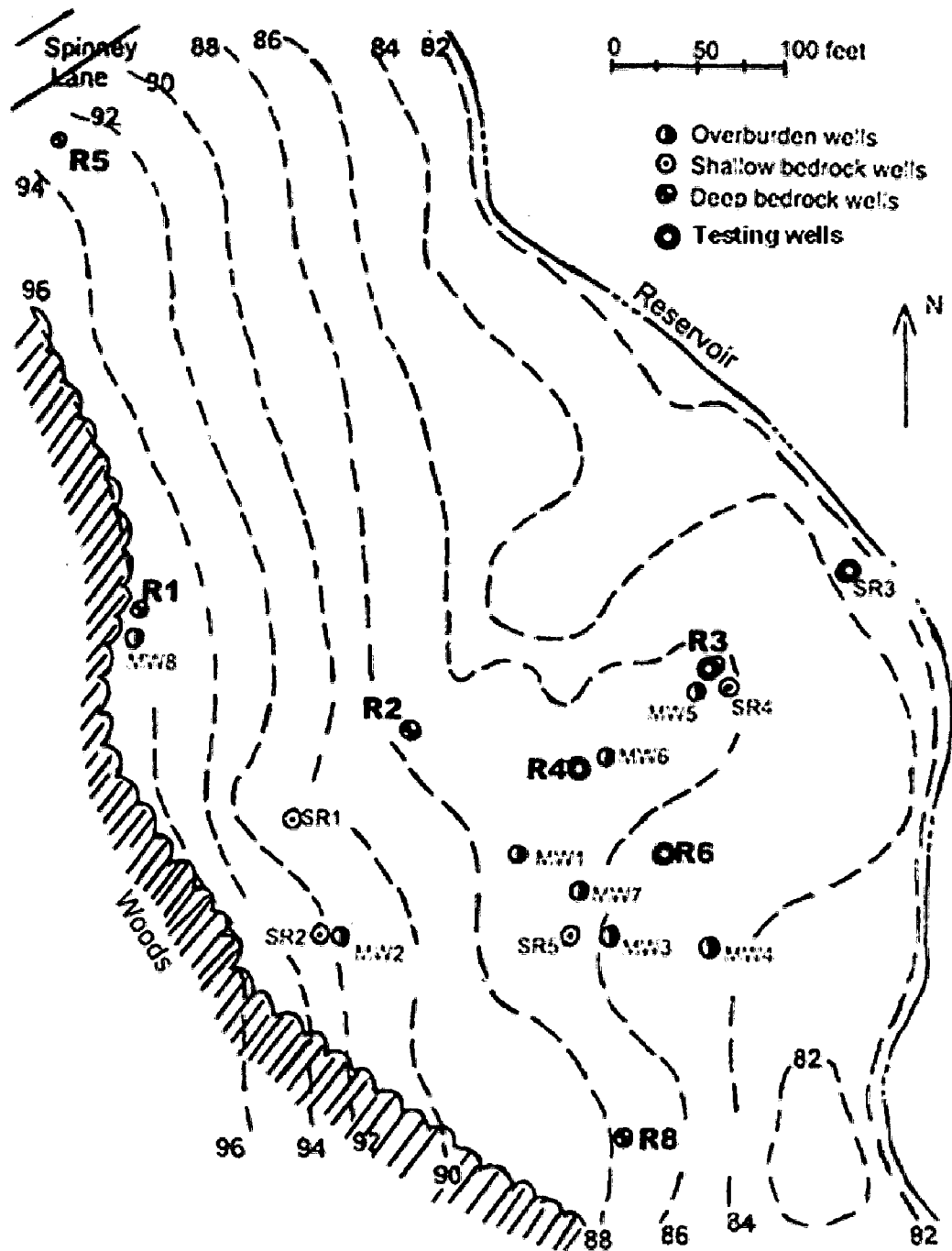
Figure 2.2 Map of UNH well field and wells used for testing. Wells used for heat injection during the dipole well test (SR3, R4 and R6) denoted by a red ring, while the pumping well (R3) is marked with a blue ring. Wells R2, R3 and R4 were also used for the single well test. Figure adapted from Helmrath (1999).

16
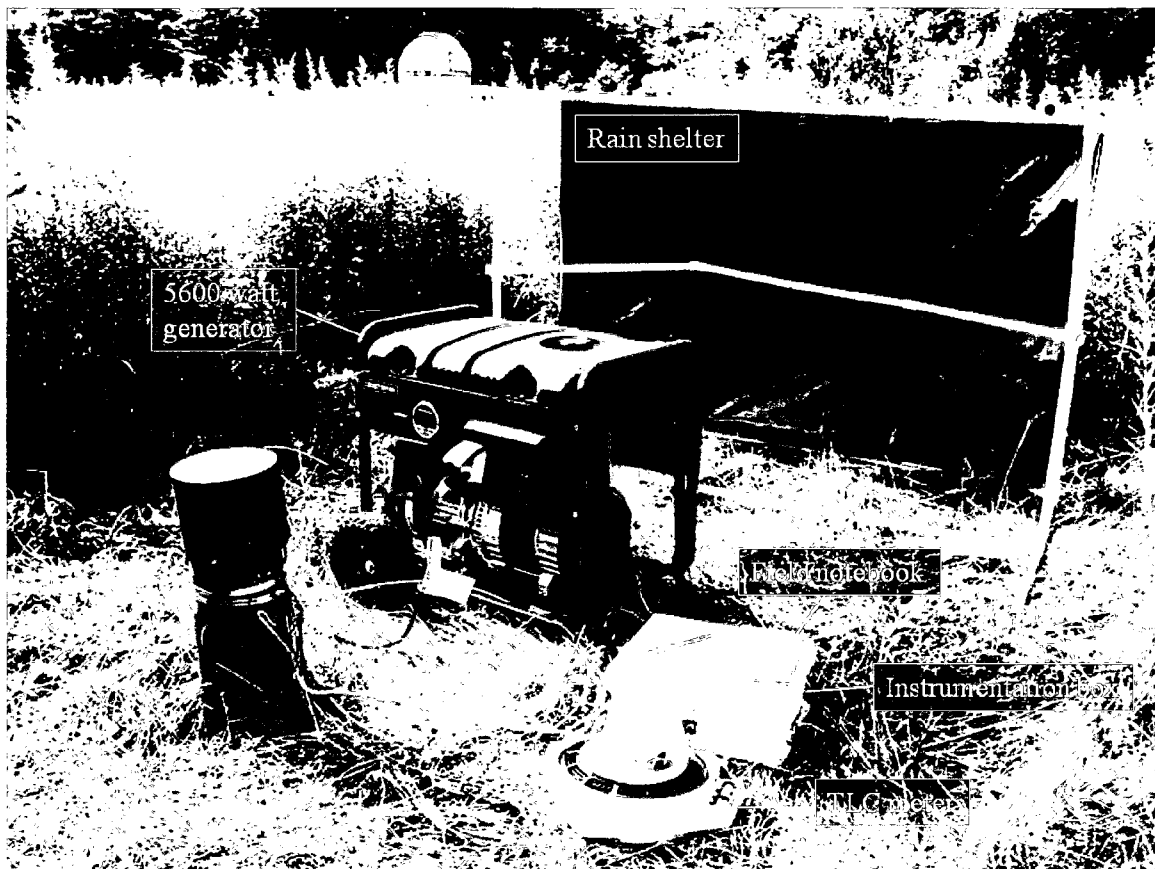
Figure 2.3 Arrangement of equipment for the single well test, in this case showing well R4. (Rain shelter removed for better view of equipment.)
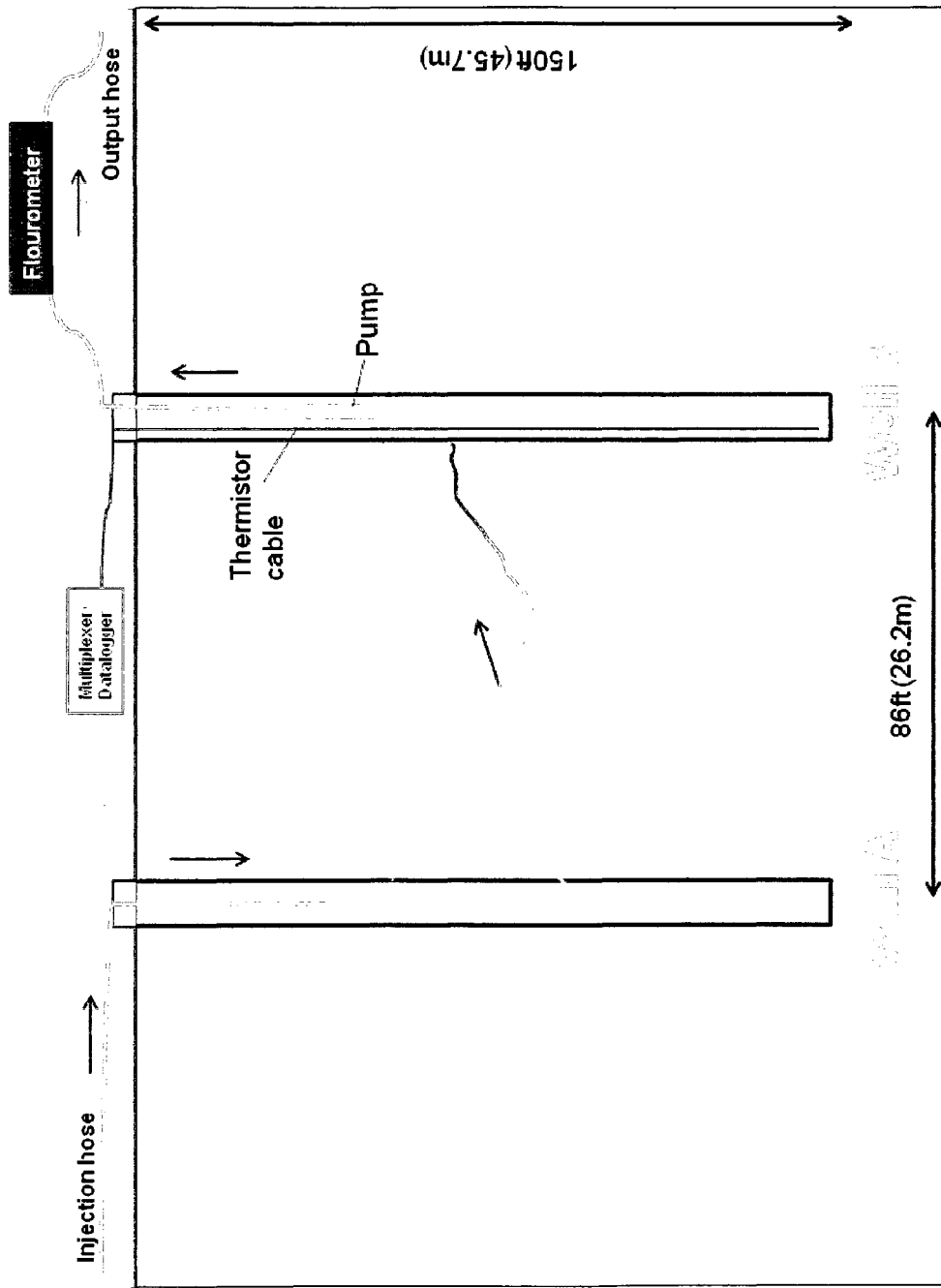
Figure 2.4 Diagram of dipole well test, showing heat injection, simplified movement of water, and thermal exchange within fractures. Equipment used in test and data collection is also shown. Black arrows indicate movement of water. (Fractures are for illustrative purposes only.)

18

CHAPTER III

RESULTS

Two varieties of thermal test were performed using the bedrock wells at the UNH well field. Each test investigates the interactions between fractured bedrock and the water within those fractures.

Single Well Test

Well R2

Prior to heating, well R2 maintained an average* temperature of 9.15 ° C. By the end of the single well test, R2 showed an increase in temperature by 2.0 °C or greater for all locations along the borehole, as shown in Figure 3.1a. An average increase of 2.19 °C was observed throughout the borehole, as shown in Figure 3.2, due to the uneven heating at some locations along the borehole. Heating in well R2 was maintained for 60 hours, however, the first five hours of data were improperly recorded due to low battery voltage on the datalogger; only the remaining 56 hours are displayed in the well profile and heating curves.

Recovery time was relatively consistent throughout, with the uppermost region of the borehole appearing to make the slowest recovery (Figure 3.1b). Throughout the

---

*All averages exclude top two sensors, because of surface fluctuations, as well as three sensors (at 110 ft, 145 ft and 150 ft) deemed erroneous.

borehole an average temperature of 9.6 °C was recovered within 21 hours after heating ceased, and 9.35 °C after 60 hours of recovery as shown in Figure 3.2. The original average background temperature of 9.15 °C was not reached during the observed recovery.

As shown in Figure 3.3, average borehole temperatures for the single well test appeared to be relatively consistent with the heat flow model, with the assumption of a thermal conductivity approximated at 2.5 W/m°C. This value, and subsequent thermal conductivities for the other single well tests, was found while matching the field data with the heat flow model curve, and maintaining the heat capacity value of 2.2 $MJm^{-3}K^{-1}$, the literature value for fractured and unfractured igneous and metamorphic rock (Signorelli, 2004).

Well R3

Prior to heating, well R3 had an average temperature of 9.57 °C. Single well test data for well R3 showed an average increase in temperature of 2.40 °C by the end of borehole heating, as seen in Figure 3.4a and 3.5. As shown in Figure 3.5, the borehole temperatures took considerably longer to rebound following some of the generator refueling periods. Heating in well R3 was maintained for 60 hours. During recovery (Figure 3.4b) an average temperature of 10.17 °C was recovered within 21 hours after heating ceased, and an average of 9.78 °C was reached after 142 hours of recovery, as shown in Figure 3.5. The previous temperature of 9.5 °C was not recovered during well observation. As shown in Figure 3.6, average borehole temperatures for the single well test appeared to be relatively consistent with the heat flow model, with the assumption of

20

a thermal conductivity approximated at 2.3 W/m°C, and heat capacity equal to 2.2 MJm^{-3}K^{-1}.

Well R4

Prior to heating, well R4 maintained an average temperature of 9.20 °C. Single well test data for well R4 showed an average increase in temperature of 2.12 °C by the end of borehole heating, as shown in Figures 3.7a and 3.8. Heating in well R4 was maintained for 60 hours.

During recovery (Figure 3.7b), an average temperature of 9.85 °C was reached within 21 hours after heating ceased, and an average of 9.52 °C was reached after 66 hours. As seen in Figure 3.8, however, the original temperature of 9.2 °C was not reached during observed recovery. Similar to R3, well R4 also showed drops in temperature surrounding periods of refueling.

As shown in Figure 3.9, average borehole temperatures for the single well test appeared to be relatively consistent with the heat flow model, with the assumption of a thermal conductivity approximated at 2.1 W/m°C, and heat capacity equal to 2.2 MJm^{-3}K^{-1}.

Dipole Well Test

Heat breakthrough was not detected in the pumping well during any of the three dipole well tests, though some tests did yield breakthrough of the tracer fluid. Steady drawdown in the observation wells during the dipole well test allowed for use of the Theim equation to calculate a transmissivity of approximately 18.92 m^2/day or 2.19 x10^{-4} m^2/sec. This transmissivity was consequently used to calculate an approximate fracture aperture of 7.06 x10^{-4} meters.

SR3 to R3

During the dipole well test between wells SR3 to R3 the pumping was maintained for 99 hours, however, the rhodamine tracer did not arrive during this period.

R4 to R3

During the dipole well test between wells R4 and R3, rhodamine arrived in the pumping well and reached a peak concentration of 41.4 ppm after 332 minutes (5.53 hours), as shown in Figure 3.10. The average residence time of the injected water was calculated to be 371 minutes for the 26.21 m surface distance between the two wells. The average flow velocity was calculated to be approximately 0.001177 m/sec (125.8 m/day).

No thermal breakthrough was observed during the 94 hours of the dipole well test (Figure 3.11). The Kolditz (1995) equation was used to model expected heat arrival using the test parameters. The calculated curve in Figure 3.14 shows that for the temperature difference of 9.6 °C between the warm reservoir water and the ambient aquifer water, thermal breakthrough of 1.0 °C is estimated to occur after 175 hours or 7 days. For the 94 hours of pumping maintained during the test, the model estimates an increase of 0.25 °C.

R6 to R3

A peak rhodamine concentration of 448 ppb arrived after 374 minutes (6.23 hours), as shown in Figure 3.12. The average residence time of the injected water was calculated as 376.7 minutes for the 32.92 m surface distance between the two wells. The average flow velocity was calculated to be approximately 0.001456 m/sec (101.7 m/day). No thermal breakthrough was observed during the 90 hours of the dipole well test between wells R6 and R3 (Figure 3.13). The calculated Kolditz (1995) curve, also in

Figure 3.14 shows that for the temperature difference of 9.6 °C between the warm

reservoir water and the ambient aquifer water, 90 hours of pumping should have yielded

a thermal breakthrough of 3.40 x10^{-3} °C. Thermal breakthrough of 1.0 °C is estimated to

occur after 436 hours, or 18 days.
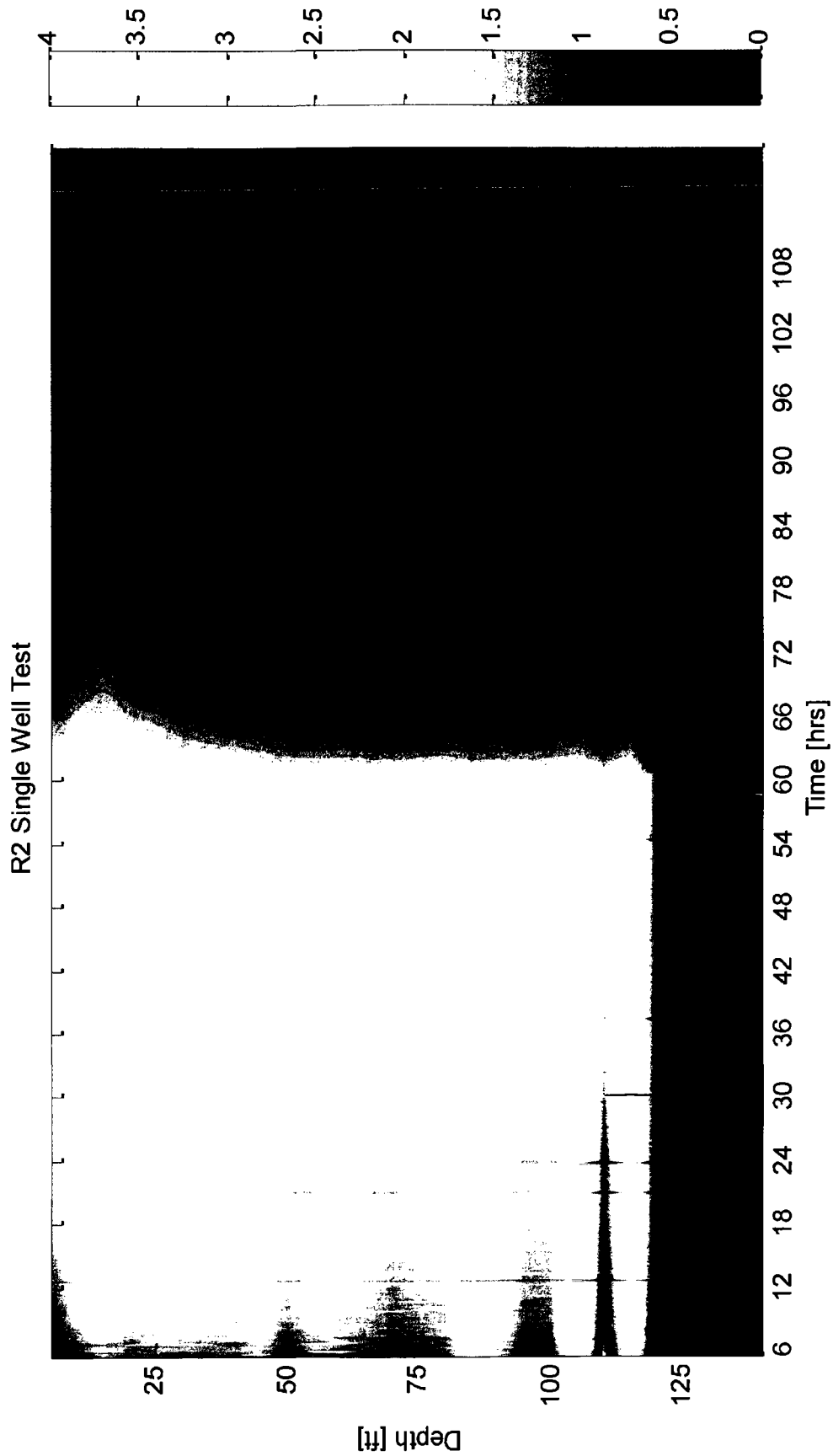
Figure 3.1a Heating profile of well R2 during the single well test. Profile shows warming of surface water due to ambient heating, as well as three distinct patches lower in the profile where the heating cable was likely in close proximity to the thermistor cable. Heating ceases at 60 hours. (Sensor at 110, 145 and 150ft are erroneous.)

Figure 3.1b Profile of well temperatures during well recovery, following 60 hours of heating. Colors indicate degrees of increase from ambient well temperature. White dashed line indicates approximate line of bedrock.

25

Figure 3.2 Heating (0 to 60 hours) and recovery (60 to 120 hours) curve of well R2 during the single well test. Time between 0 and 5 hours was lost due to voltage error. Outlying low temperature points likely caused by periods of refueling.

26

Figure 3.3 Heat flow approximation of temperature decrease over time (red squares) compared with actual temperature recovery data from R2 single well test (blue diamonds). Heat capacity (K) was estimated to be 2.5 W/m°C and heat capacity to be 2.2 MJm^{-3}K^{-1}.
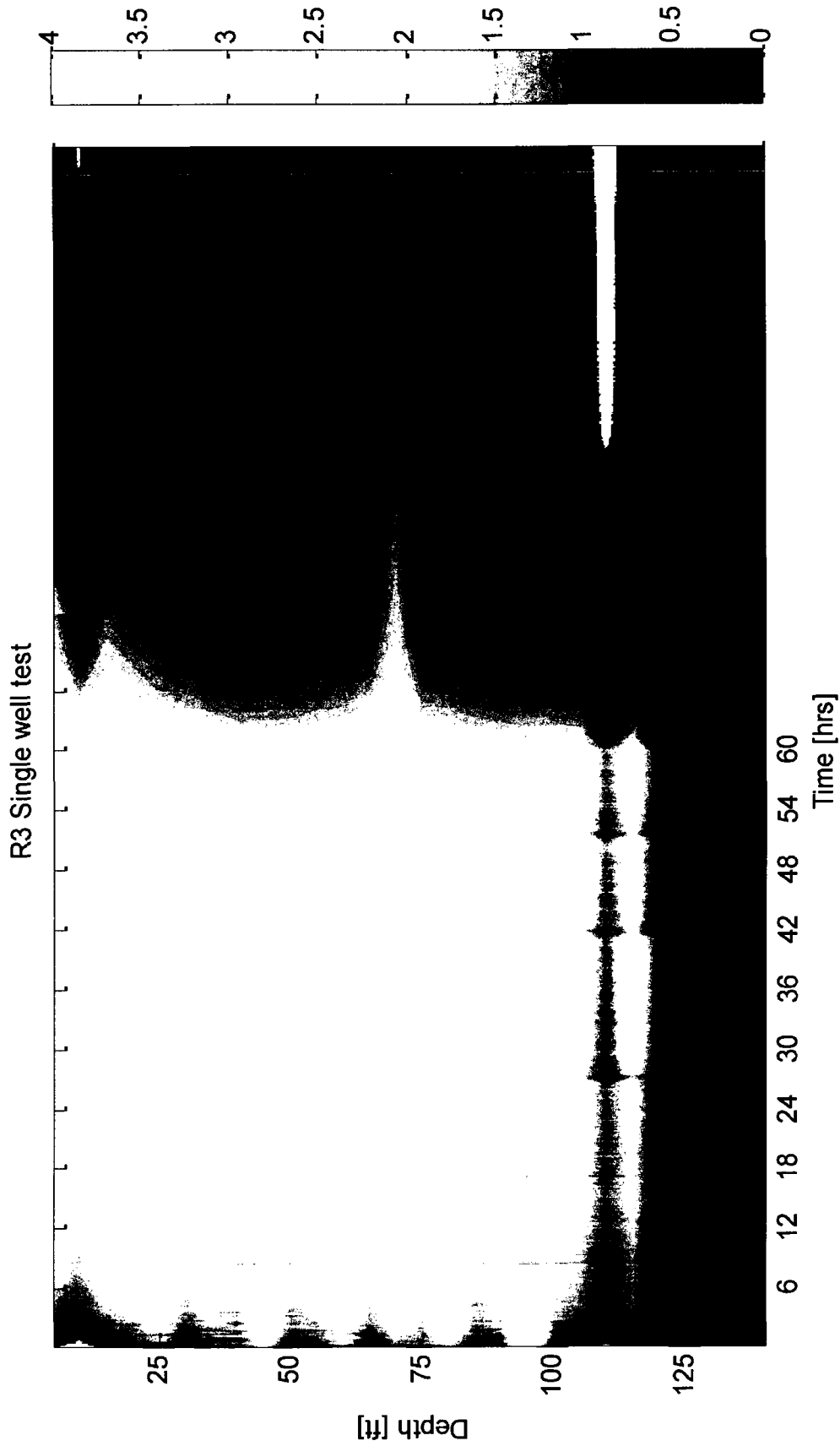
Figure 3.4a Heating profile of well R3 during the single well test showing increase in temperature. Borehole heating occurs between time zero and 60 hours (beyond 60 hours is recovery). Profile shows relatively even heating besides a few locations where the heating cable may have been in closer proximity to the thermistor cable. (Sensor at 110, 145, and 150 ft are erroneous.)
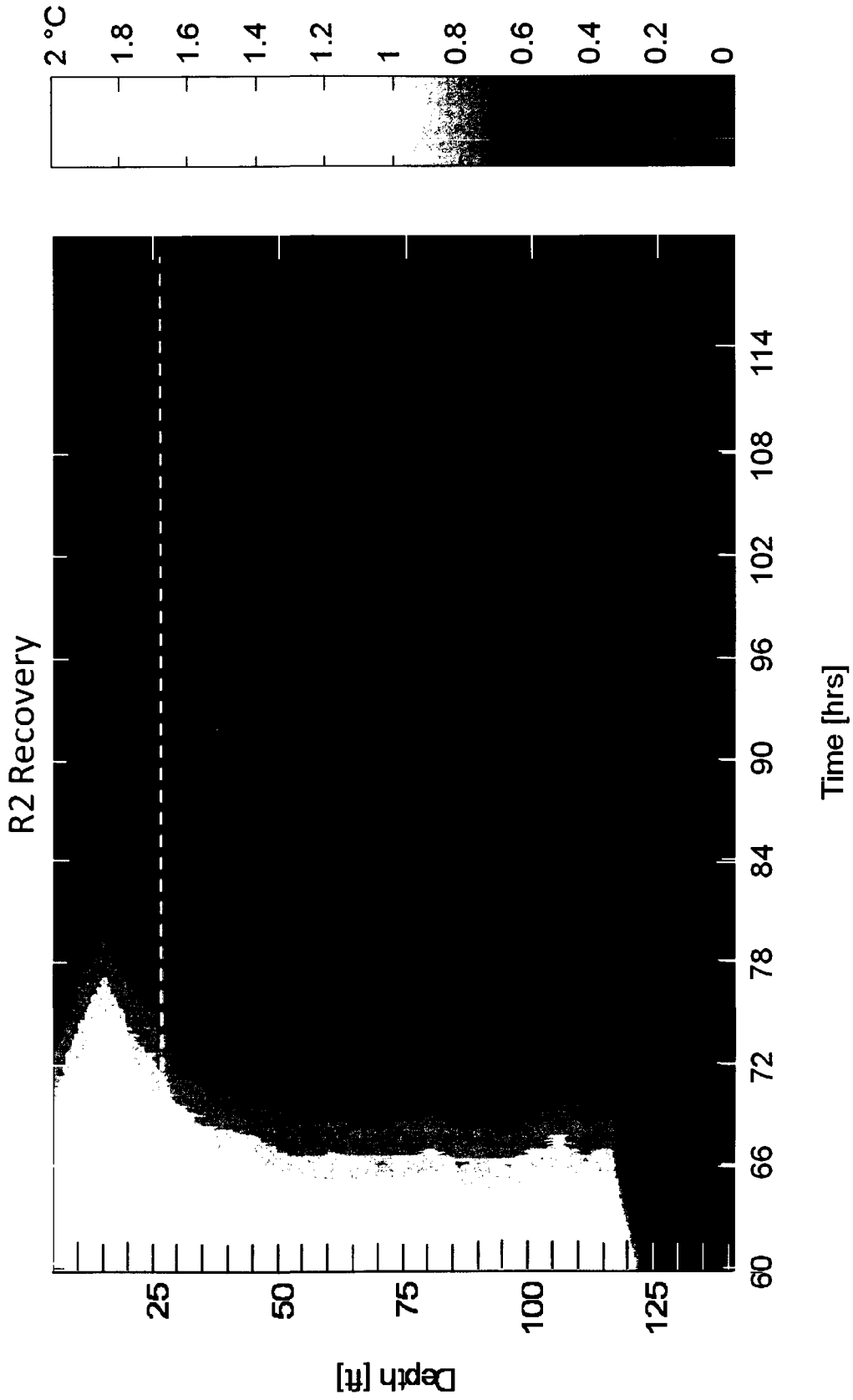
28
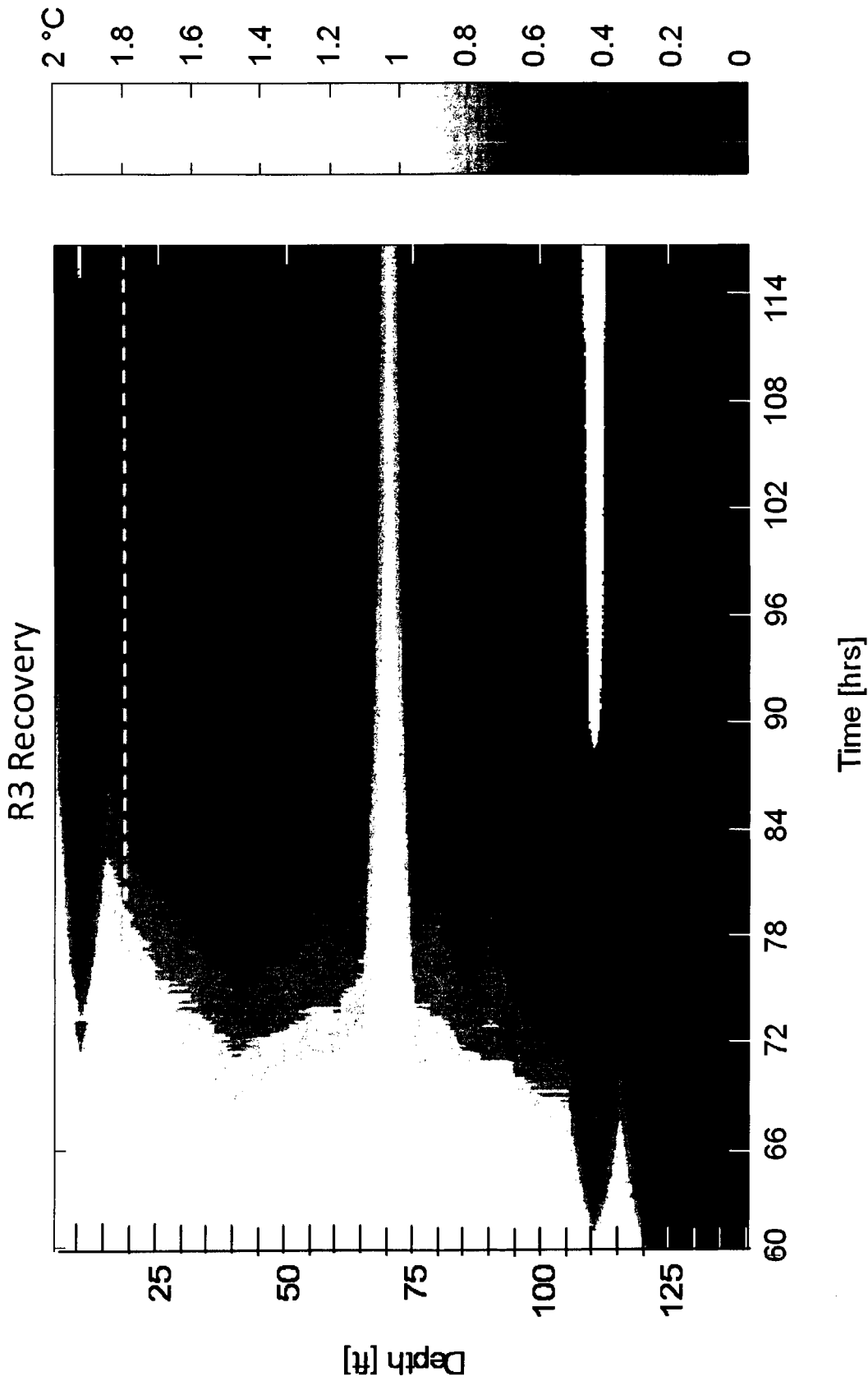
Figure 3.4b Profile of well temperatures during well recovery, following 60 hours of heating. Colors indicate degrees of increase from ambient well temperature. White dashed line indicates approximate line of bedrock.
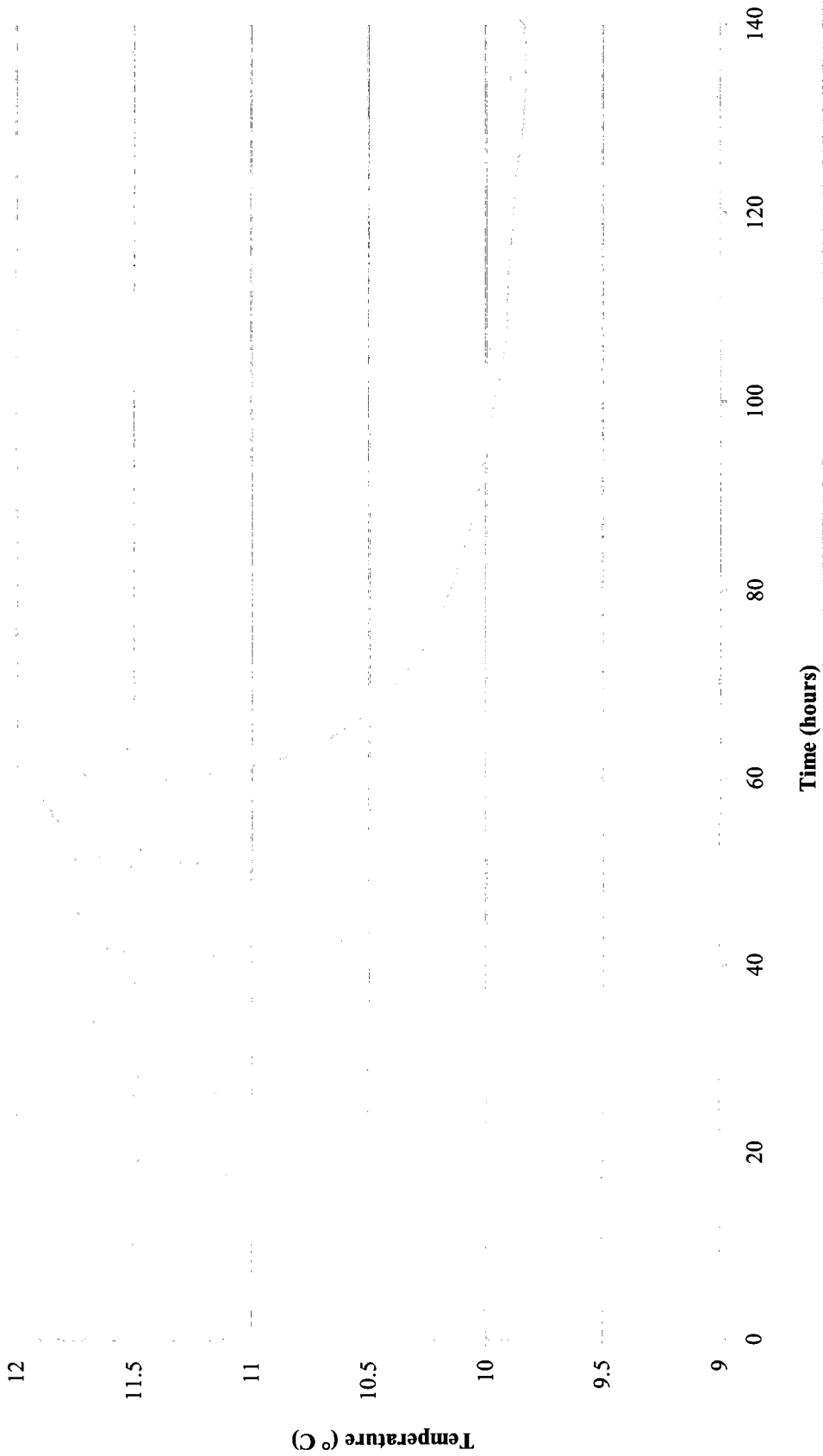
Figure 3.5 Heating (0 to 60 hours) and recovery (60 to 140 hours) curve of well R3 during the single well test. Outlying low temperature points likely caused by periods of refueling.
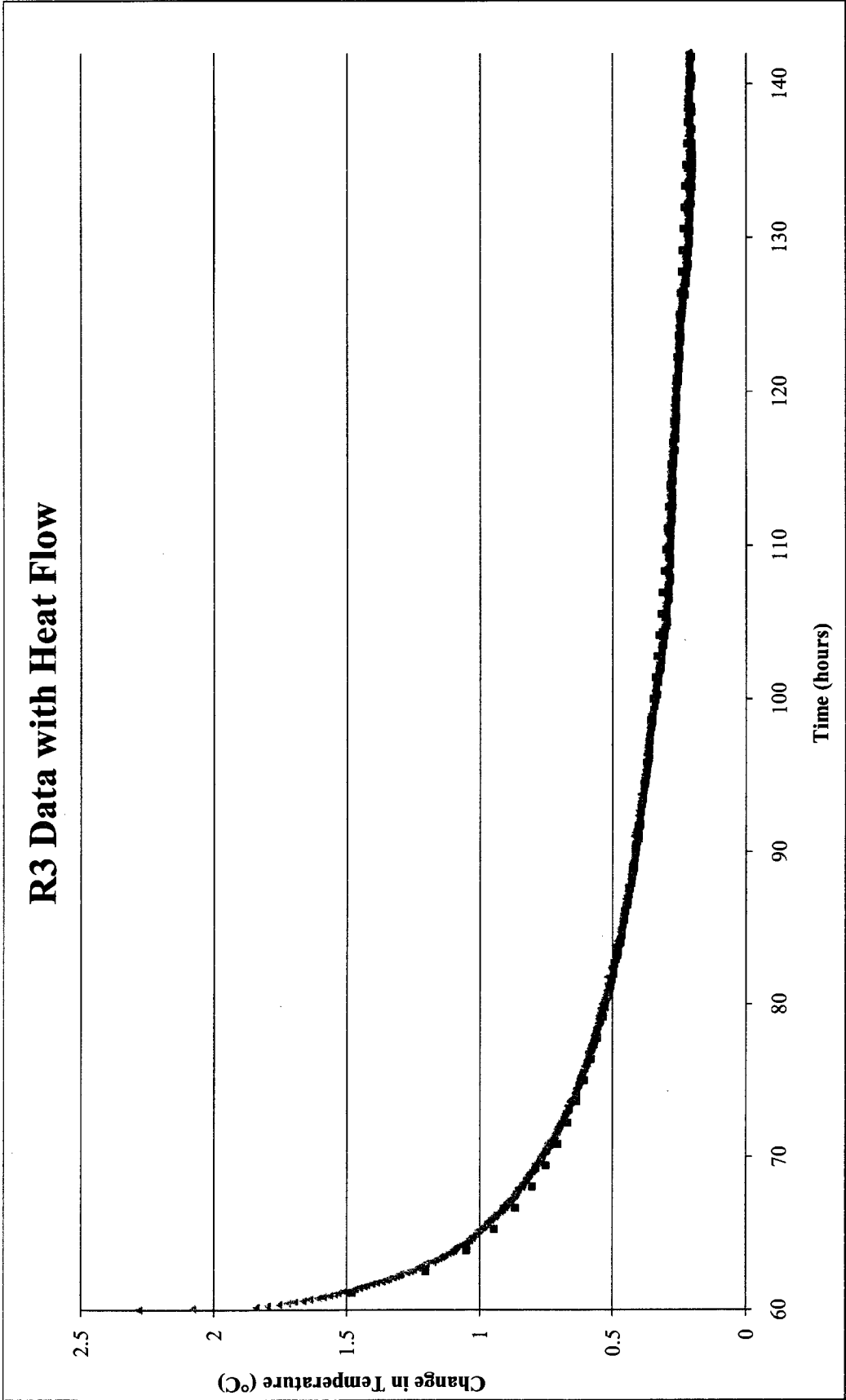
Figure 3.6 Heat flow approximation of temperature decrease over time (red squares) compared with actual temperature recovery data from R3 single well test (green triangles). Thermal conductivity (K) is estimated to be 2.3 W/m°C and heat capacity to be 2.2 MJm^{-3}K^{-1}.
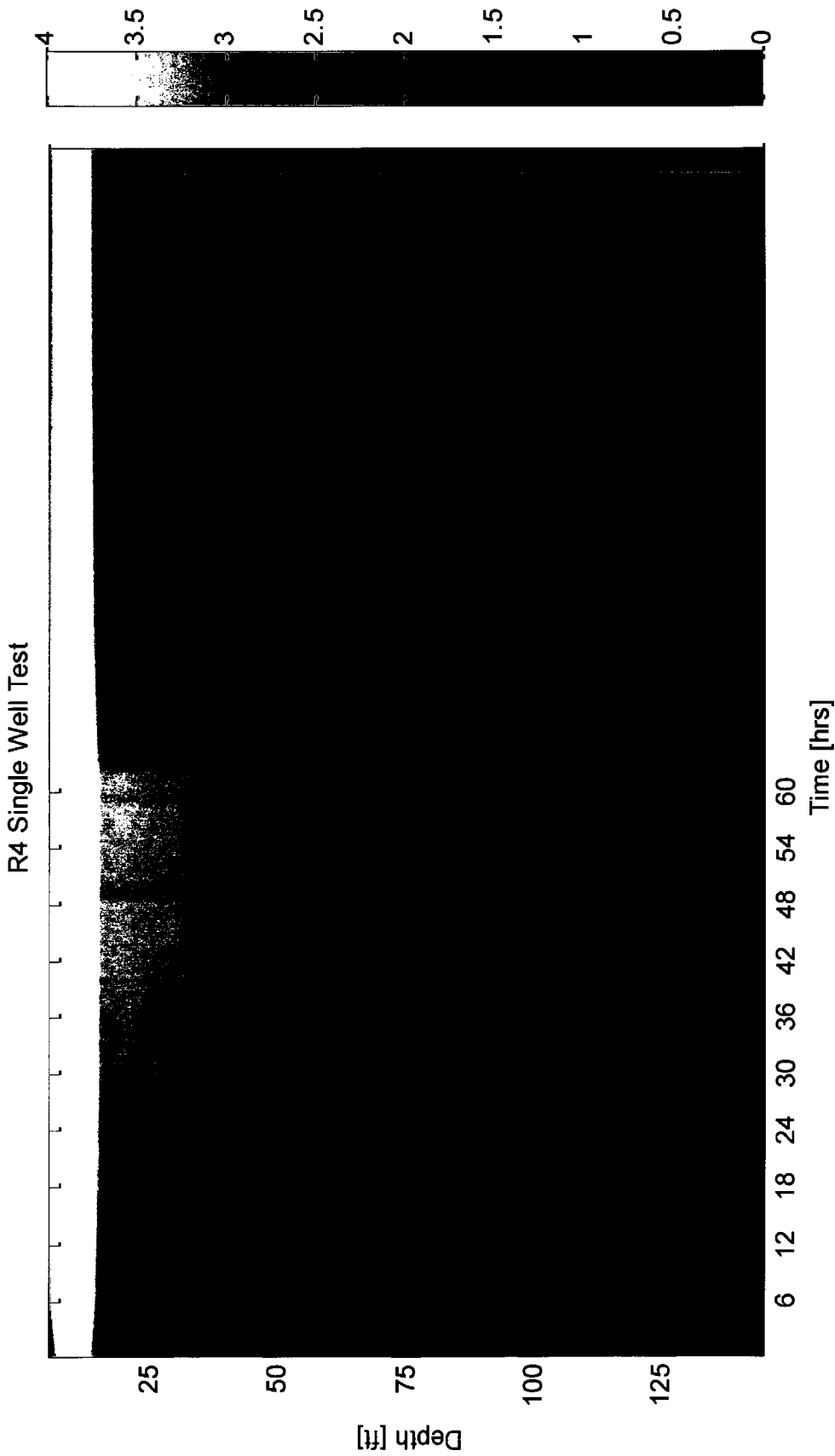
Figure 3.7a Heating profile of well R4 during the single well test. Borehole heating occurs between time between zero and 60 hours (Time beyond 60 hours is recovery). Profile shows relatively consistent heating throughout borehole, and warming of surface water due to ambient heating during early July. (Sensor at 110, 145 and 150 ft are erroneous.)
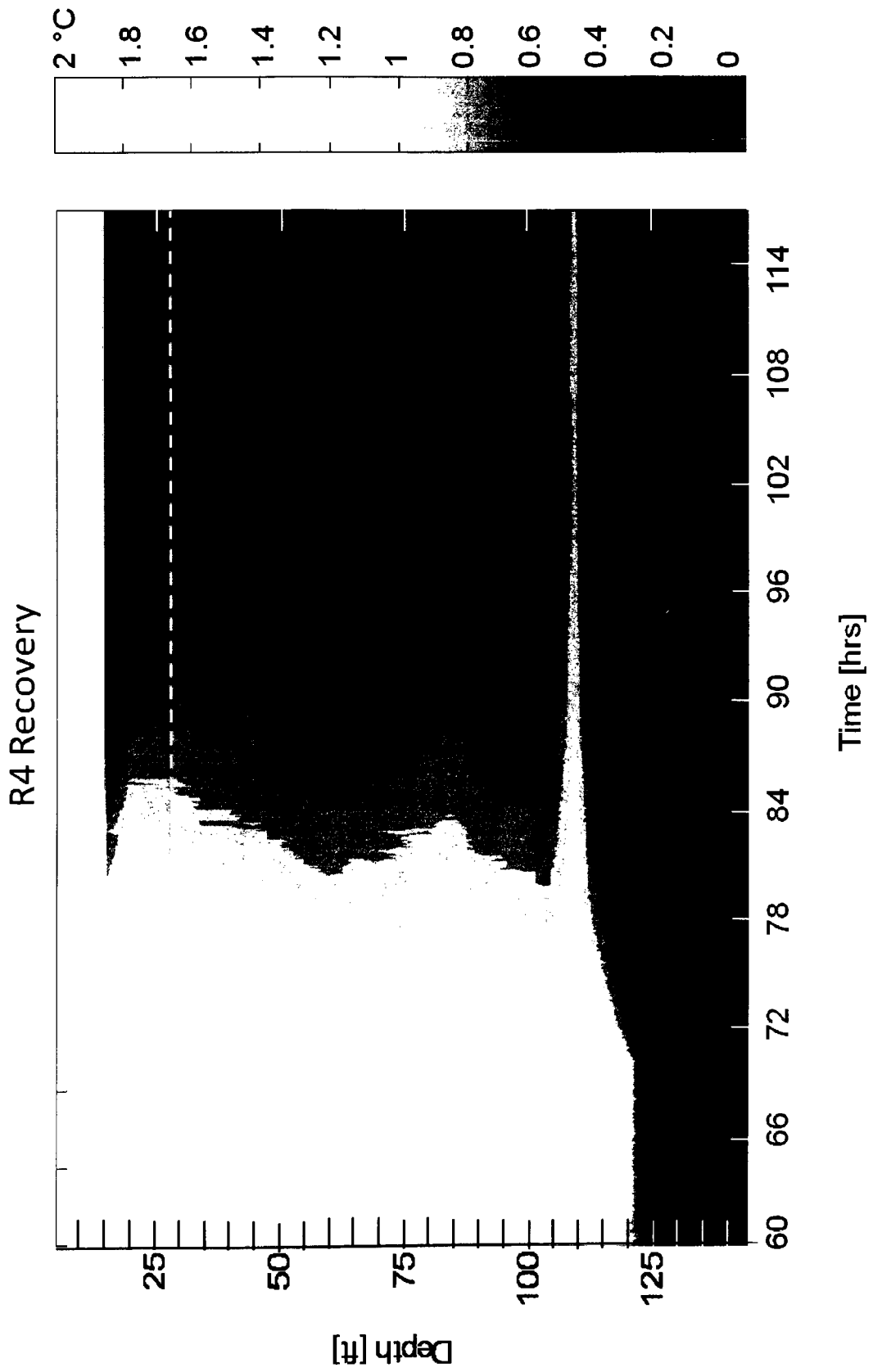
Figure 3.7b Profile of well temperatures during well recovery, following 60 hours of heating. Colors indicate degrees of increase from ambient well temperature. White dashed line indicates approximate line of bedrock.
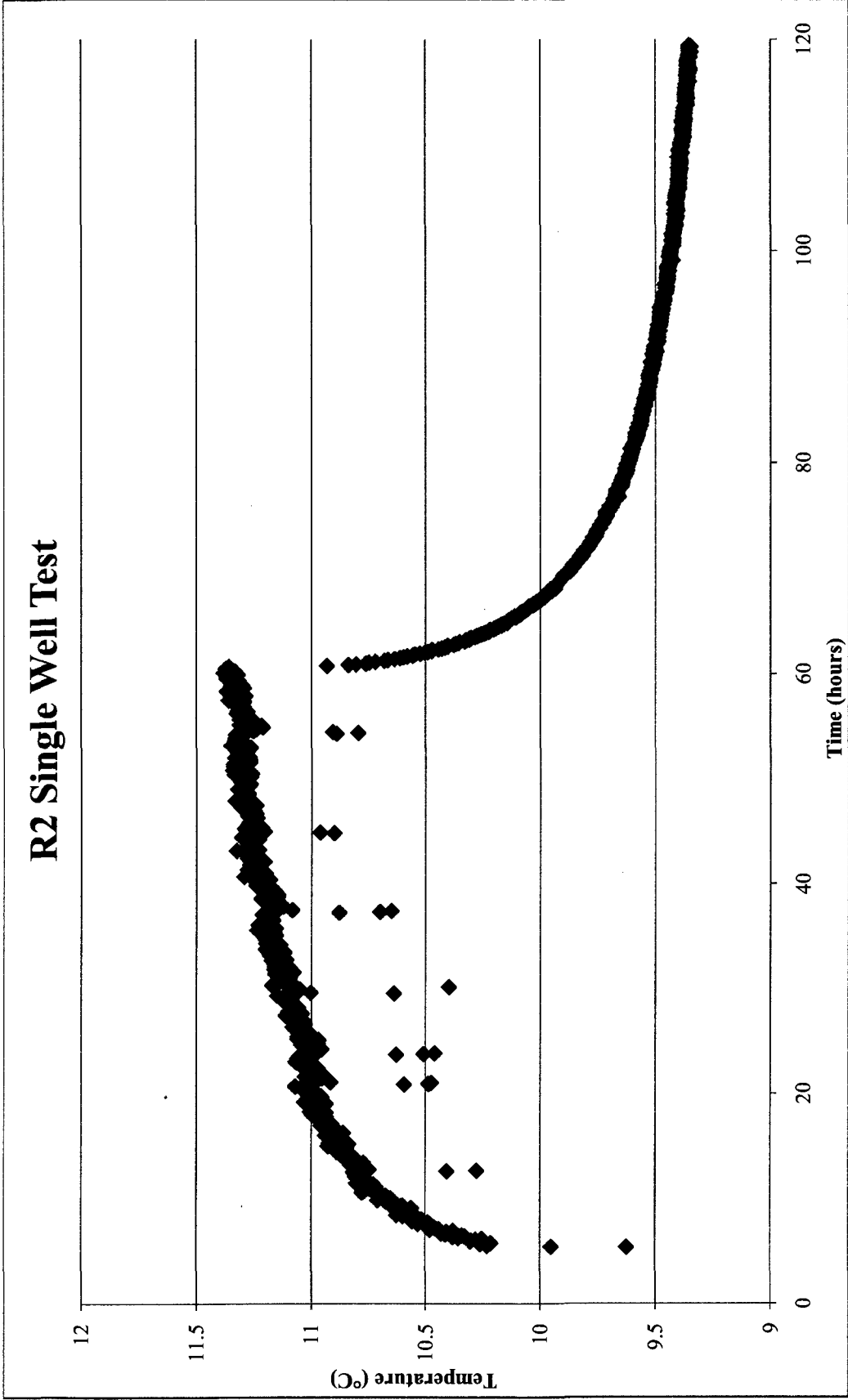
33
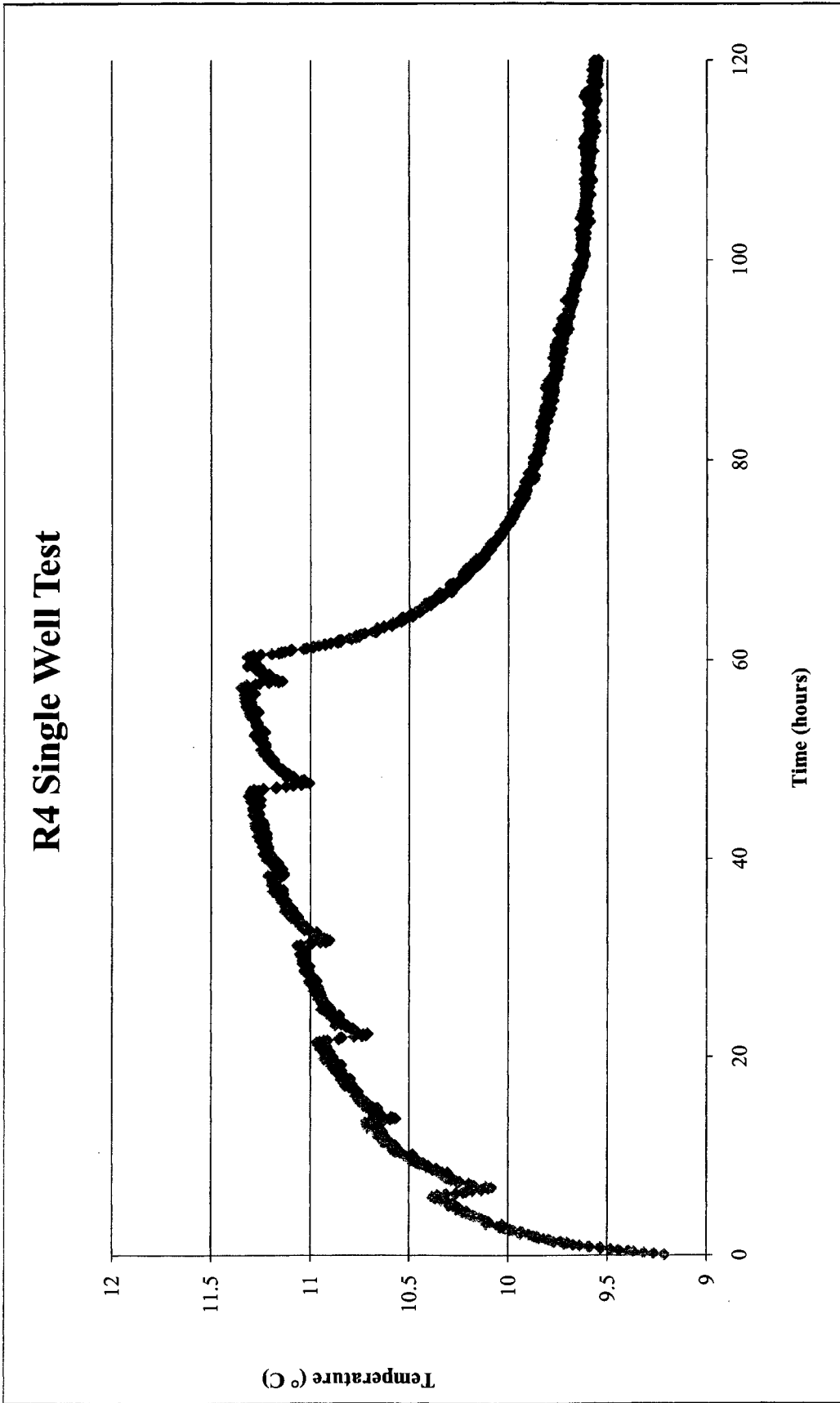
Figure 3.8 Heating (0 to 60 hours) and recovery (60 to 120 hours) curve of well R4 during the single well test. Outlying low temperature points likely caused by periods of refueling.
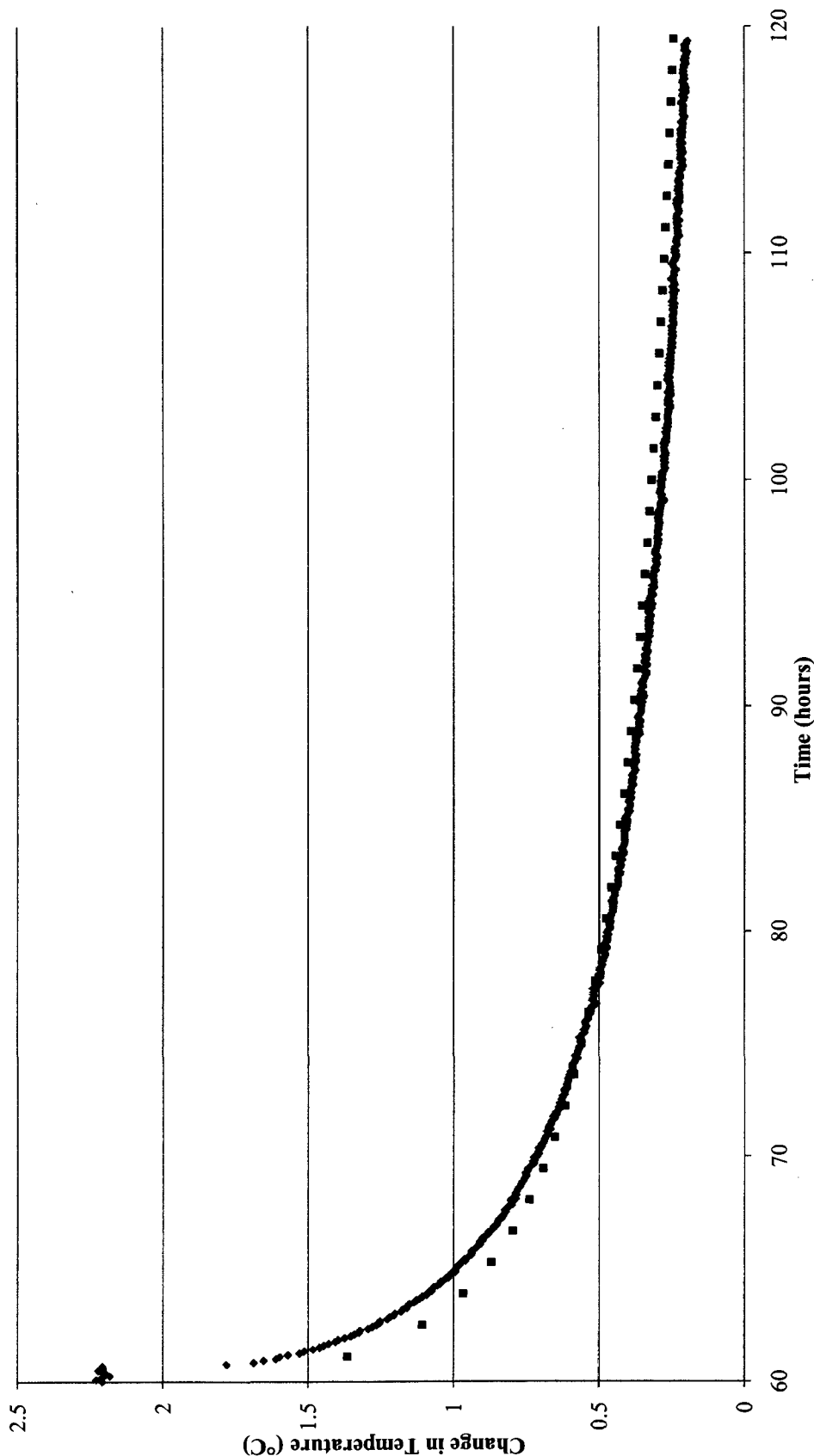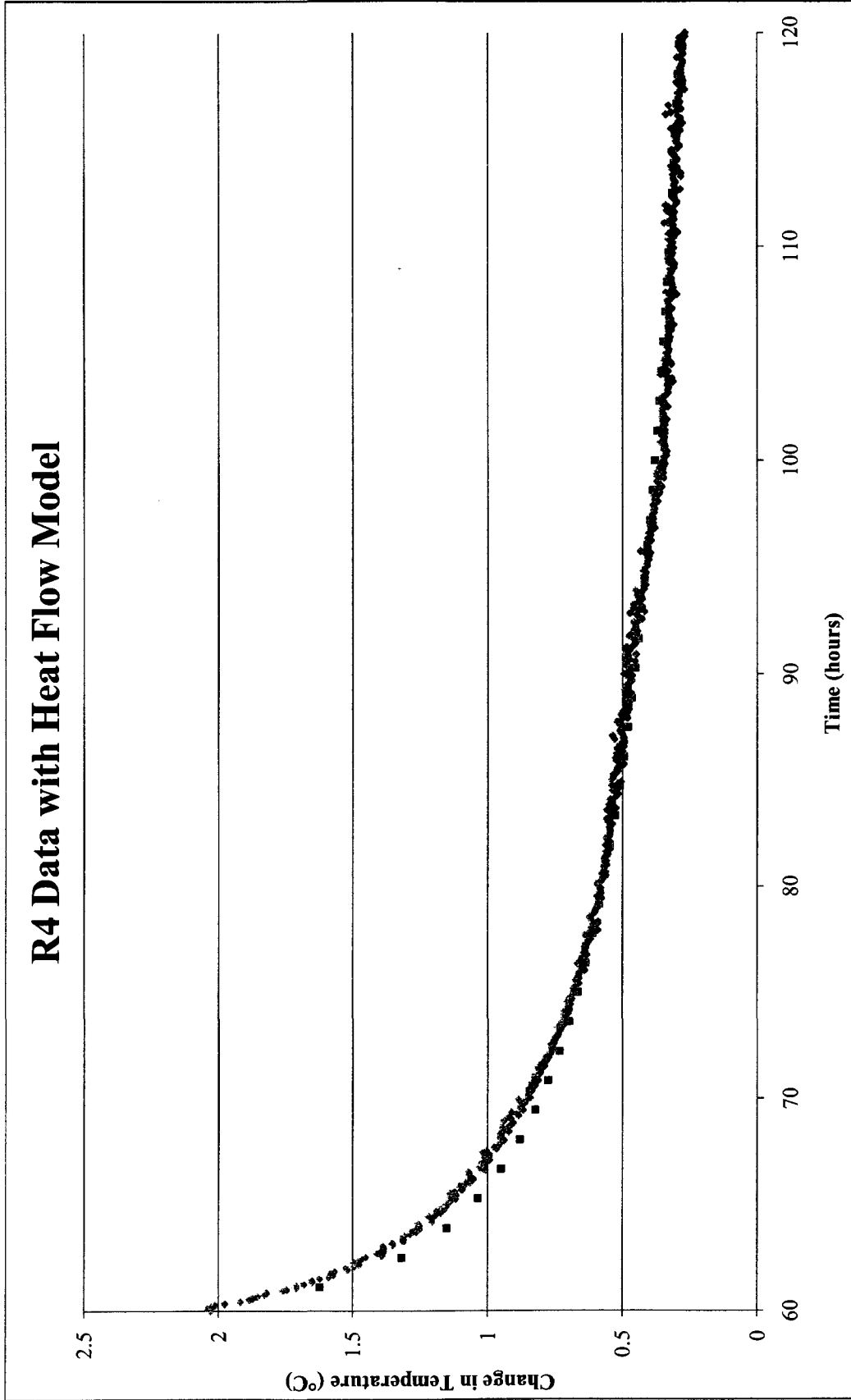
Figure 3.9 Heat flow approximation of temperature increase over time (red squares) compared with actual temperature data from R4 single well test (orange diamonds). Thermal conductivity (K) is estimated to be 2.1 W/m°C and heat capacity to be 2.2 $MJm^{-3}K^{-1}$.
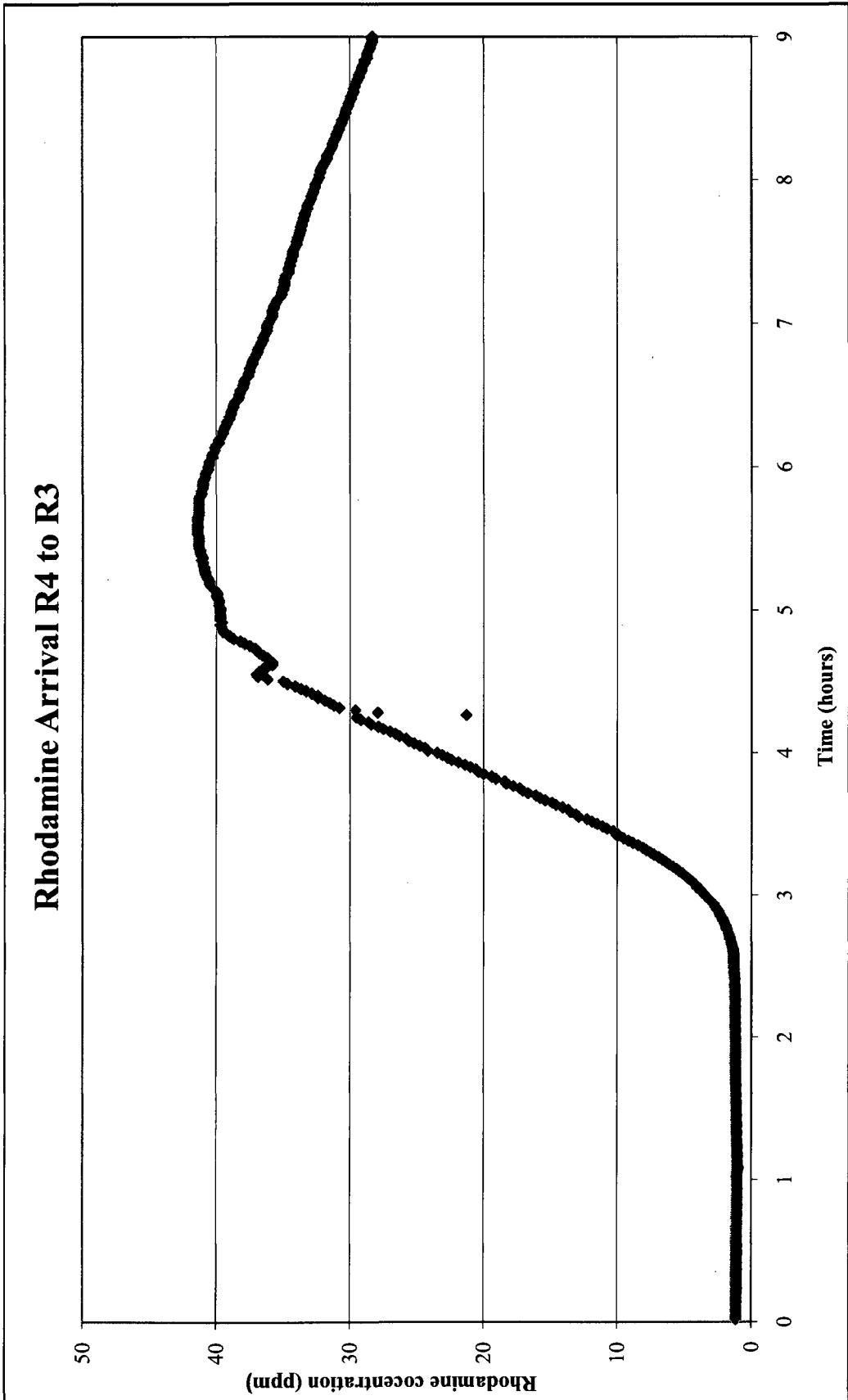
Figure 3.10 Arrival curve of rhodamine during dipole test R4 to R3. Concentration in parts per million, time measured as hours from injection into well R4 increase.

36
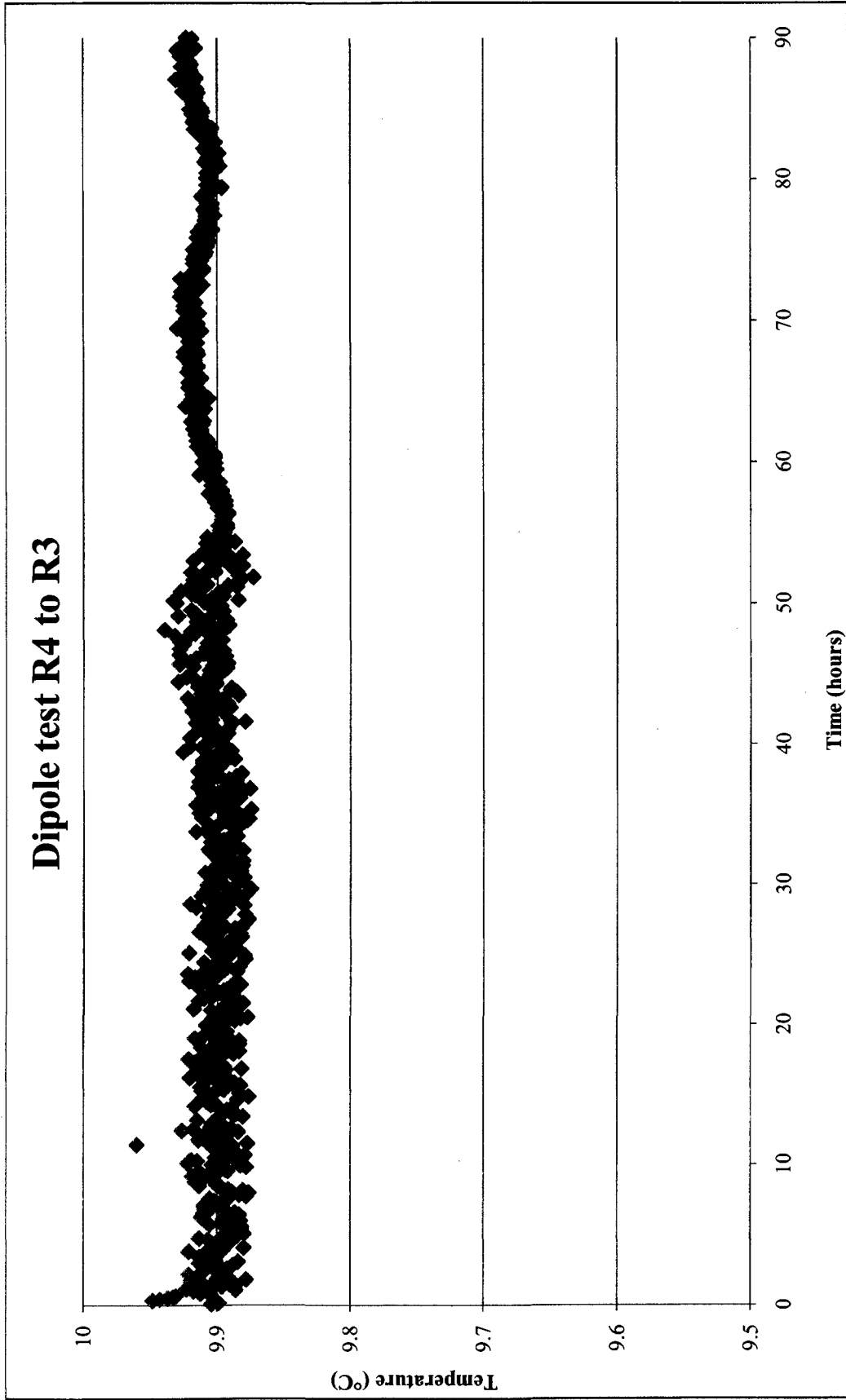
Figure 3.11   Average borehole temperature in well R3 during the dipole well test between R4 and R3.   Test was performed for 94 hours.
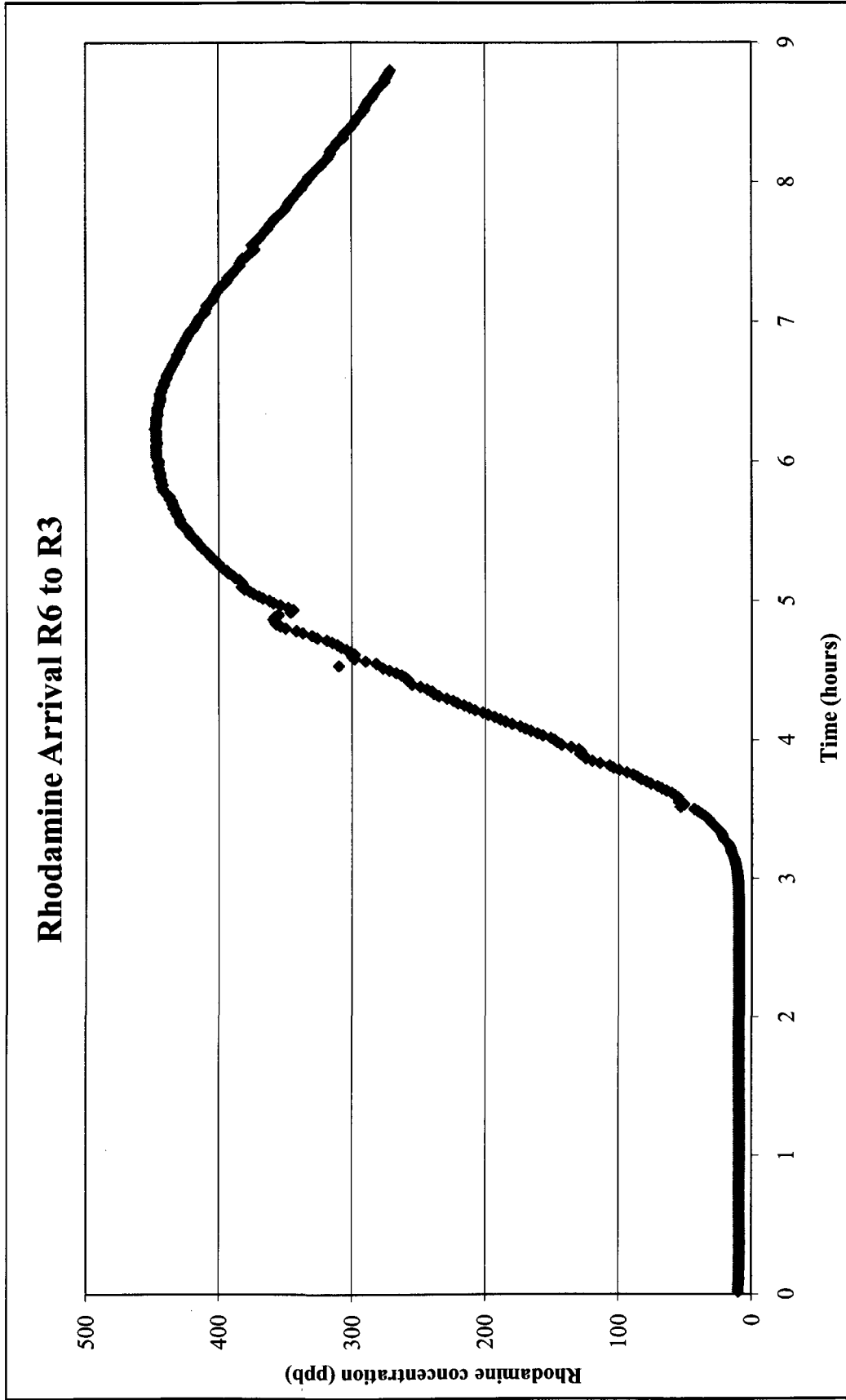
Figure 3.12 Arrival curve of rhodamine during dipole test R6 to R3. Concentration in parts per million, time measured as hours from injection into well R6 increase.
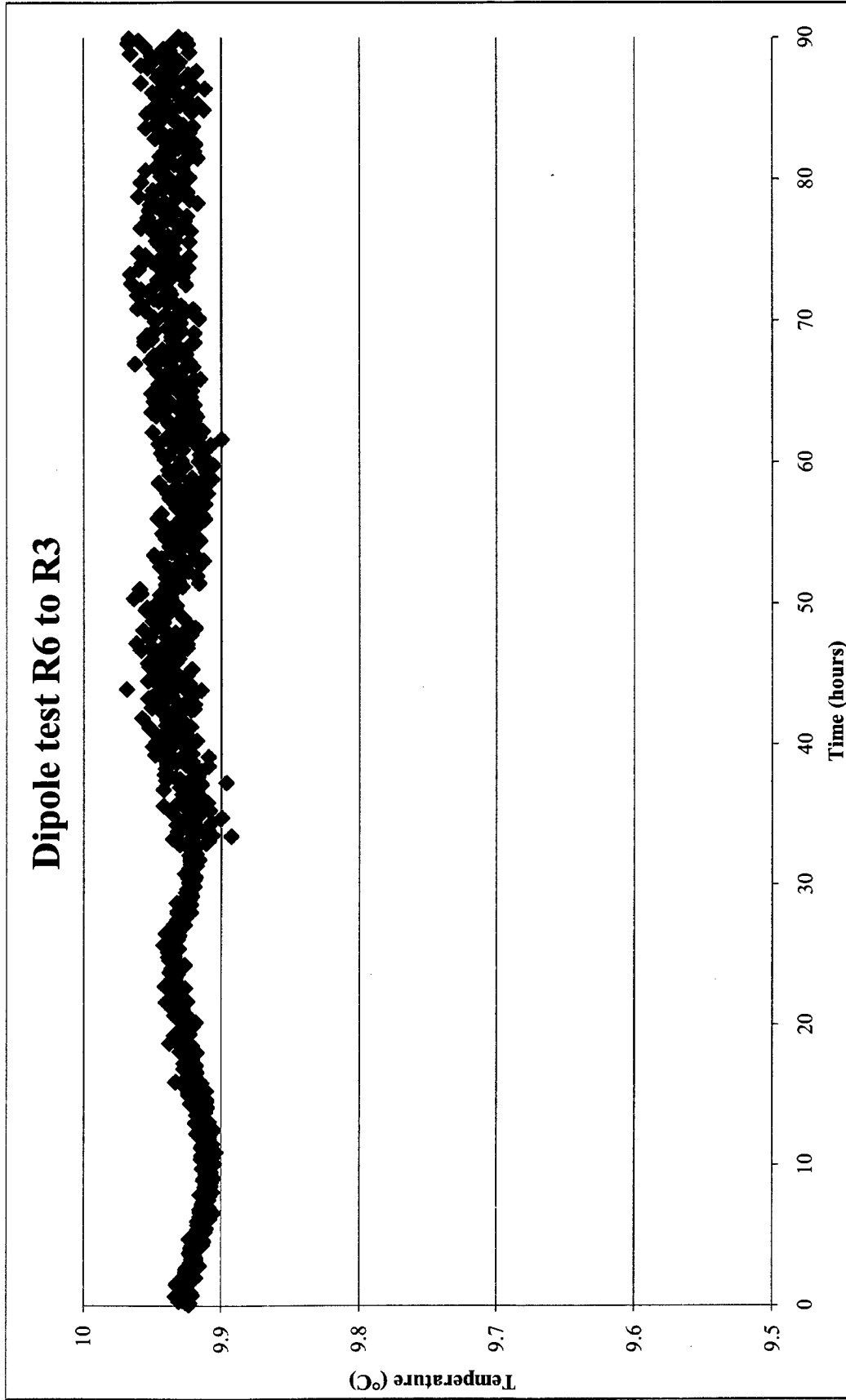
Figure 3.13 Average borehole temperature in well R3 during the dipole well test between R6 and R3. Test was performed for 90 hours.
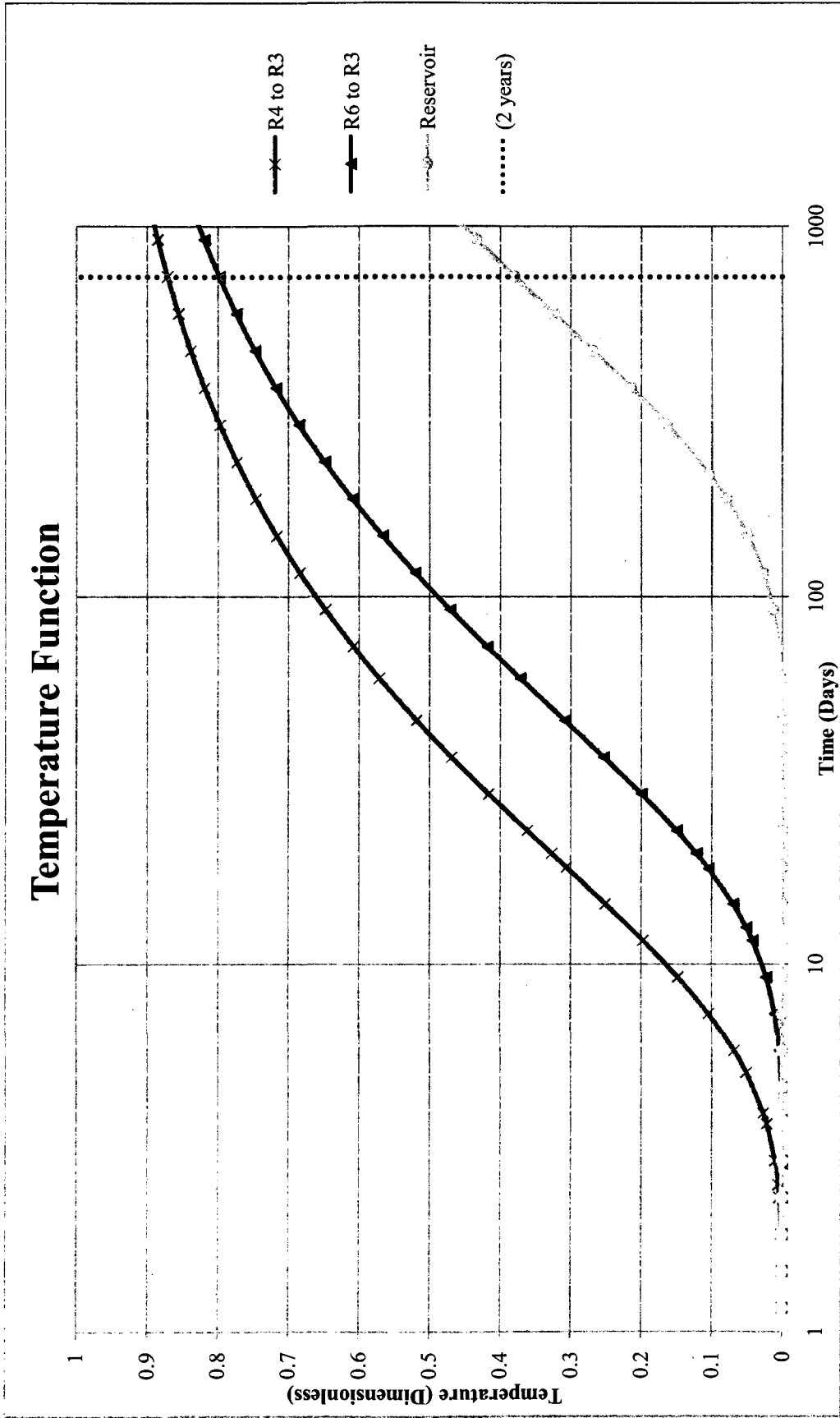
Figure 3.14 Thermal breakthrough curve based on Kolditz (1995) equation. Dimensionless temperature modeled versus days at the pumping well R3 for a dipole arrangement between well R3 and three different wells. Well R4, having a distance of 26.21 meters (86 ft); well R6, having a distance of 32.92 meters (108 ft); and the reservoir 30.48 meters (100 ft) away.

CHAPTER IV

DISCUSSION

This discussion presents the findings of the single and dipole well tests, as they reveal both site specific information and patterns relevant to SCWs in general. The first section deals with the single well test, comparing each data set to the appropriate model in order approximate both thermal conductivity and heat capacity. The second section addresses the dipole well test, and what it brings to light concerning fracture aperture, fluid velocity, and thermal properties. The last section discusses the ramifications of this research for the sustainability of the residential use of SCW systems.

Single Well Test

During each of the single well tests, the collected data showed more intense heating in the overburden. This region also had a distinctly slower recovery, compared to the remaining borehole profile, during all three single well tests. This response can be attributed to the lower heat capacity surface materials (Signorelli, 2004), causing more rapid heating and higher temperature in the surrounding water because less heat is able to travel into the material surrounding that portion of the borehole.

During heating, well profiles (Figures 3.1a, 3.4a and 3.7a) show patches of more intensely raised temperature throughout the borehole, particularly in well R3; this may be attributed to differences in the proximity of the thermistor cable to the heating cable. The

more significant portion of the temperature record, the recovery period, is the most insightful place to make comparisons and observe temperature differences.

For well R2, recovery was relatively consistent below the bedrock area and showed no regions of dramatically slowed cooling. From drilling records, well R2 is known to not be hydraulically conductive, however, anomalies in the borehole radar were identified at three locations by Foster (2000) who assumed them to be fractures (Table 4.1). The fracture identified by Foster (2000) near 80 ft lines up with an area of slightly retarded cooling within the R2 single well profile, as shown in Figure 3.1b. The other fractures identified by Foster (2000) within R2 are unfortunately near the erroneous sensor (110 ft) and below the level of borehole heating, which only stretched to 120 ft. Other areas of slightly slowed cooling evident in Figure 3.1b may be caused by regions of slightly reduced thermal conductivity, but do not line up with identified borehole radar anomalies.

Table 4.1 Approximate depth of fractures in well R2, above 120 ft, as measured by Foster (2000) using borehole radar.

Depth (m)	Depth (ft)
24.8	81.4
33.3	109.3

For well R3, recovery within the bedrock showed multiple areas where cooling was distinctly slowed. At 55 ft cooling is only slightly delayed, which may correlate with the borehole radar anomaly observed by Foster (2000) at 47.6 ft (Table 4.2), but is some distance away. The other two fractures locations observed by Foster (2000) within the heated region of R3 show distinctly retarded cooling, as shown in Figure 3.4b.

Table 4.2 Approximate depth of fractures in well R3, above 120 ft, as measured by Foster (2000) using borehole radar.

Depth (m)	Depth (ft)
14.5	47.6
21	68.9
27.4	89.9

Well R4 also shows delayed recovery at areas matching borehole radar anomalies observed by Foster (2000) (Table 4.3). Slowed cooling is evident near 80 ft (Figure 3.7b), as well as at 115 ft, though the later is somewhat obscured by the erroneous sensor at 110 ft.

Table 4.3 Approximate depth of fractures in well R4, above 120 ft, as measured by Foster (2000) using borehole radar.

Depth (m)	Depth (ft)
24.7	81.0
35.1	115.2

Though these locations were identified by Foster (2000) as bedrock fractures, this study only reveals these areas to be regions of anomalous thermal characteristics. Enhanced cooling, which was expected at fracture locations prior to testing, was not observed during any of the recovery periods. Most likely thermal conductivity at each of these points is lower than the surrounding bedrock, but this is not necessarily caused by the presence of a fracture at each location. The presence of mineral veins with a lower thermal conductivity could also cause anomalies at those locations.

Curve matching with the heat flow model for each single well test approximates thermal conductivity to be 2.5 W/m°C for well R2, 2.3 W/m°C for well R3, and 2.1 W/m°C for well R4. The average thermal conductivity for the three tests is 2.3 W/m°C, while heat capacity is equal to 2.2 $MJm^{-3}K^{-1}$. This average is lower than the documented value of thermal conductivity of 2.6 W/m°C for the Exeter Diorite (Roy et al., 1968). It

is possible that the effective thermal conductivity of the fractured bedrock is distinctly lower than that of the unfractured bedrock. Additionally, the thermal conductivity documented by Roy et al. (1968), was measured in a lab situation on individual samples and may have created conditions to yield different results than in situ testing.

Dipole Well Test

Though some drawdown occurred in well SR4 during pumping of well R3, failure for the tracer dye to arrive in the pumping well during the dipole well test between well SR4 and R3 indicates these wells to be only distally hydraulically connected.

The tracer test between well R4 and R3 allowed a calculation of the average fluid velocity of 125.8 m/day. The tracer test between well R6 and R3 allowed a calculation of the average fluid velocity of 101.7 m/day. Considering the average flow velocities of the two dipole well tests are similar, it is likely the water is flowing through a simple fracture network. The wells may lie upon different points of the same fracture or a small number of connected fractures.

The fact that thermal breakthrough did not occur during any of the dipole well tests, despite the arrival of the tracer dye, indicates heat exchange at the surfaces of the fractured crystalline bedrock to have been great enough that all heat was taken up prior to the water arriving in the pumping well. The absence of thermal breakthrough also appears to be consistent with the Gringarten and Sauty (1975) model, particularly in that the injection rate during this research was less than the withdrawal, creating only a weak dipole. Most residential scale SCW systems would have a pumping rate significantly lower than that used during this research. With heating season estimated at 5 months each year, average pumping rates would be closer to 7.36×10^{-5} m^3/s (Deng, 2000).

Larger scale systems, such as office buildings would have higher pumping rates, closer to 5.89×10^{-4} m^3/s (Deng, 2000), and may also have ambient/injected water temperature differences greater than those estimated for this research. Even with these large scale systems, the rate of thermal breakthrough would be slightly retarded compared to that modeled in Figure 4.1. Since the Kolditz (1995) equation was designed for a dipole well set where the rate of injection was equal to the rate of pumping, the time of thermal breakthrough calculated by this model underestimates the actual time for these conditions. For the tests performed during this research the rate of injection was many times lower than the rate of withdrawal; most SCWs would be set up similarly.

Implications for Standing Column Wells

The Kolditz (1995) equation can also be used to model the thermal breakthrough derived from a recharge boundary. In Figure 3.14, the models of each of the dipole tests is compared to a hypothetical dipole test between well R3 and a body of water 100 ft (30.48 m) away, the distance between the pumping well and the old Durham reservoir. The only difference between each of the tests in modeled in Figure 3.14 is the distance from the point of injection to the pumping well. The dipole from R3 to the reservoir is modeled as an image well located 200 ft from the pumping well.

For a constant pumping rate matching that used during testing (4.08×10^{-4} m^3/s), and 9.6 °C of water temperature difference between the pumping well and the reservoir, thermal breakthrough (1.0 °C) is calculated to occur after 5111 hours or 213 days (Figure 3.14). Thus, it would not have been possible for thermal breakthrough from the Old Durham reservoir to have interfered with the dipole well testing during this research. The

temperature change approximated by this model (Figure 3.14) for each of the dipole well tests is listed in Table 4.4.

Table 4.4 Tabulated results of the Kolditz (1995) model for each of the dipole well tests.

Test	Distance to pumping well	1.0 °C of change after	0.5 °C of change after
R4 to R3	26.21 meters (86 ft)	7 days	5 days
R6 to R3	32.92 meters (108 ft)	18 days	13 days
Reservoir to R3	30.48 meters (100 ft)	213 days	148 days

Actual SCW systems are more accurately represented when a limited number of annual months of heating are assumed (pumping occurs only during heating season), yielding a lower annual average pumping rate. Therefore, Figure 4.1 shows the temperature curves of three hypothetical SCW systems with all conditions the same except for pumping rates, which are estimated based on each building type.

Each hypothetical SCW is located 100 ft (30.48 m) from a surface water body that has a temperature 9.6 °C cooler than the ambient water in the fractures. Each system is only active for 5 months of annual heating, and no pumping occurs during the remaining 7 months of the year. During the heating season the pumping will draw cold water into the fractures, gradually cooling the pumped water and reducing the heating efficiency of the SCW system. Changes in absolute temperature are approximated using the Kolditz (1995) model.

The first system, utilized in a hypothetical office building, has an annual average pumping rate of 5.89 x 10^{-4} m^3/s, or 1.38 x 10^{-3} m^3/s during heating months as described by Deng (2000). For this system, a decrease of 1.0 °C would is seen after approximately 148 days. After a period of 10 years with the same conditions, 7.4 °C of temperature

decrease is approximated; after 30 years, 8.2°C. The approximated temperature changes

for this system, as well as the other theoretical SCW systems are listed in Table 4.5.

Table 4.5 Results of the Kolditz (1995) model for each theoretical SCW system in Figure 4.1.

Theoretical system	Pumping rate	1.0 °C of change after	Temperature change after 10 years	Temperature change after 30 years
Office building	5.89×10^{-4} m^3/s (1.38×10^{-3} m^3/s or 22 gpm during heating)	148 days	7.4 °C	8.2 °C
Field Well (R3)	1.73×10^{-4} m^3/s (4.08×10^{-4} m^3/s or 6.47 gpm during heating)	515 days	5.2 °C	7.0 °C
Residential	7.36×10^{-5} m^3/s (1.73×10^{-4} m^3/s or 2.75 gpm during heating)	1181 days	3.6 °C	5.9 °C

Though the Gringarten and Sauty (1975) model and Kolditz (1995) modification

are not perfectly fitted for the field conditions in this research, they are still useful for

estimating the type of heating trend that could be experienced over the life of a SCW

system. Because of the weak dipole configuration of the dipole well tests, the model

underestimates heat arrival due to its assumptions concerning injection rates. However,

when applied to a constant temperature boundary condition such as that of a nearby

surface water body, the model clearly illustrates that significant temperature change will

be observed in the pumping well over time. Depending on the temperature difference in

ambient and injected/recharge water, the distance between the pumping well and

injection/recharge area, the fracture aperture, and the pumping rate; thermal breakthrough

even half as large as that modeled could be significant. The most effect would be seen on

SCW systems installed within aquifers barely meeting the heat requirements. Those

systems may begin to lose efficiency because of the bleed, which is implemented to

increase efficiency in the first place. Additionally, in aquifers where multiple SCW systems, drinking water or agricultural wells, or nearby recharge areas are present, the effect of bleed upon the thermal change would be compounded. The theoretical SCW systems modeled in Figure 4.1 only considered body of water 100 ft away, but for many SCW systems the reinjection or disposal of thermally depleted water may be significantly closer to the pumping well.
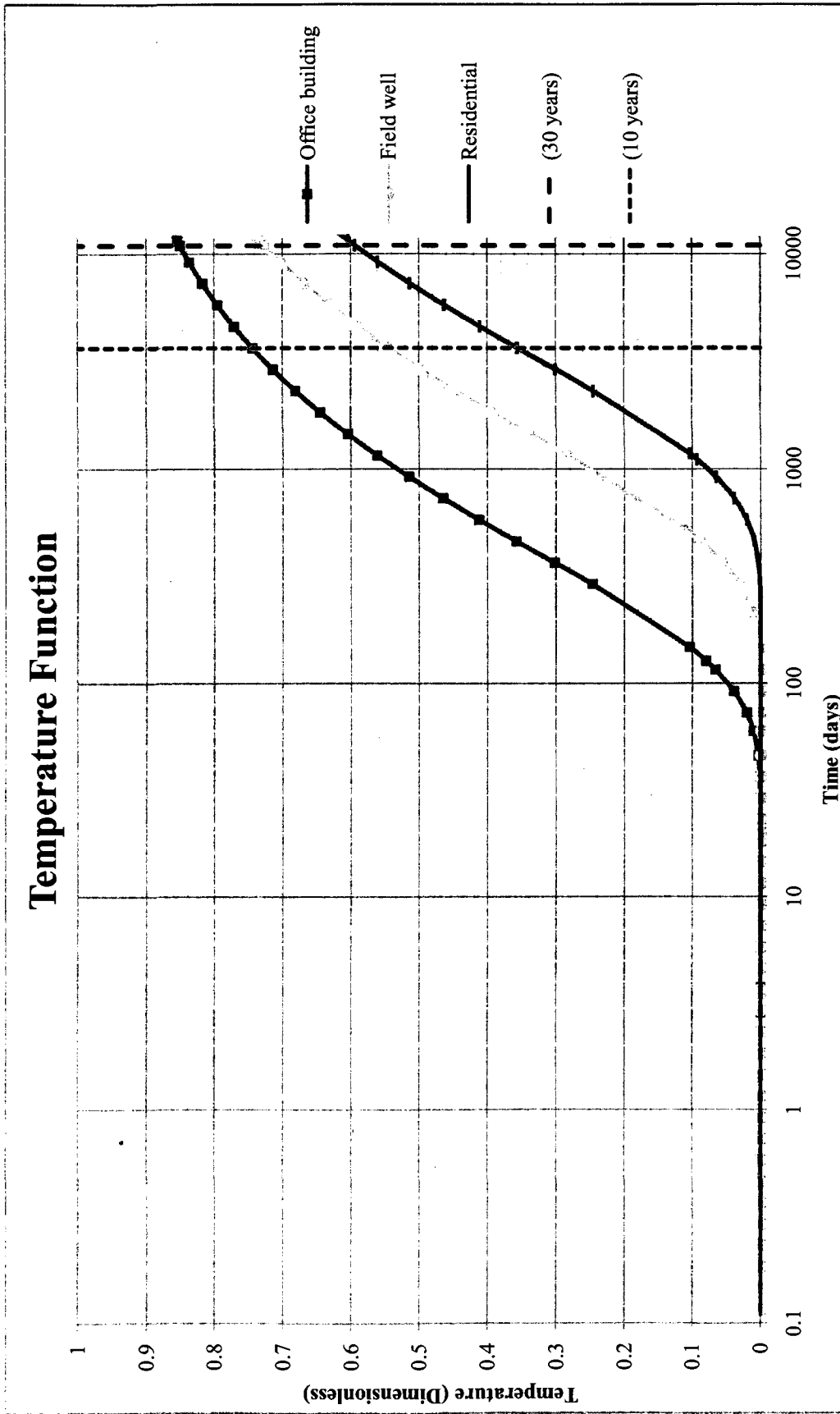
Figure 4.1 Thermal breakthrough curve based on Kolditz (1995) equation. Dimensionless temperature modeled versus days for three theoretical SCW applications. Each curve is modeled considering the annual average pumping rate of each system, assuming 5 months of heating (5 months of pumping) per year.

CHAPTER V

CONCLUSIONS

The two methods of field test used in this research facilitate the assessment of certain heat parameters and fracture characteristics. The single well heating test allows for the potential identification of fractures or otherwise thermally anomalous regions playing a role in thermal transport to and from a borehole. The identity of these locations as hydraulically conductive fractures could be investigated in further studies using a packer test. During a packer test a pump would be isolated at the top and bottom by inflatable packers and then lowered to the section of borehole in question; allowing this region to be isolated while its hydraulic yield is quantified.

Additional comparison with a heat flow model allows single well test data to be used to estimate effective thermal conductivity and heat capacity. If one of the two parameters is already known, the other is more likely to be estimated accurately. Continual checks of heat output equipment and calibration of temperature sensing instruments would add another layer of accuracy to these measurements.

The use of rhodamine tracer during the dipole well test allows the fluid velocity to be calculated in a relatively straight forward manner. This portion of the test also revealed a single fracture connection between test wells R3, R4 and R6; and an approximate aperture of this fracture.

The heat injection portion of the dipole well test provides data comparable to the temperature curve created using the Kolditz (1995) equation, but this comparison would be more manageable under conditions where a thermal breakthrough is expected after a shorter time period. Helpful test modifications may include a larger difference in ambient and injected water, closer well spacing, or a higher pumping rate.

Modeling using the Kolditz (1995) equation aid understanding in how the various heat parameters and setup conditions could affect the long term efficiency of a SCW system. When certain well spacing and pumping rates are being considered prior to an installation, this knowledge could be a vital tool.

Suggestions for Future Work

This research brings to light a number of ways in which the effective heat exchange within fractured bedrock could be more thoroughly investigated. First, the Gringarten and Sauty (1975) model and the Kolditz (1995) variation would be more appropriately applied to a dipole couplet where the rate of injection was equal to the rate of withdrawal. Second, a higher pumping rate, though not reflective of a SCW system, would allow thermal breakthrough data to be compared to the model in a more consistent manner. This would allow assessment of its applicability to a single fracture as in the Kolditz (1995) variation, compared the original Gringarten and Sauty (1975) model, which dealt with an entire aquifer.

On a longer time scale, thermal observations of actual residential and commercial scale SCWs with and without nearby reinjection of water would further confirm the applicability of the Gringarten and Sauty (1975) and Kolditz (1995) models to these systems.

LIST OF REFRENCES

Deng, Z. 2000. Modeling of Standing Column Wells in Ground Source Heat Pump Systems. *Ph.D. Thesis, Oklahoma State University,* 304pp.

Ferguson, G. 2006. Potential use of particle tracking in the analysis of low-temperature geothermal developments. *Geothermics.* 35: 44–58.

Foster, P.J. 2000. The application of surface and borehole ground penetrating radar to characterize surficial deposits and bedrock fracture in the seacoast. *M.S. Thesis, University of New Hampshire,* 136pp.

Gringarten, A.C and J.P. Sauty. 1975. A Theoretical Study of Heat Extraction From Aquifers With Uniform Regional Flow. *Journal of Geophysical Research.* 80(35): 4956-4962.

Gul, I.H. and A. Maqsood. 2006. Thermophysical Properties of Diorites along the Prediction of Thermal Conductivity from Porosity and Density Data. *International Journal of Thermophysics.* 27 (2): 614-626.

Helmrath, E.K. 1999. The Stratigraphy of the UNH Hydrology Research Site, in Durham, New Hampshire. *M.S. Thesis, University of New Hampshire,* 91pp

Kocabas, I. 2005. Geothermal reservoir characterization via thermal injection backflow and interwell tracer testing. *Geothermics.* 34 :27-46.

Kolditz, O. 1995. Modelling Flow and Heat Transfer in Fractured Rocks: Dimensional Effect of Matrix Heat Diffusion. *Geothermics.* 24(3):421-437.

O'Neill, Z. D., Spitler, J. D., and S.J. Rees. 2006. Performance Analysis of Standing Column Well Ground Heat Exchanger Systems. *American Society of Heating, Refrigerating and Air-Conditioning Engineers, Inc. (ASHRAE)* 112(2):633-643.

Rees, S. J., Spitler, J. D., Deng, Z., et al. 2004. A Study of Geothermal Heat Pump and Standing Column Well Performance. *ASHRAE*. 110(1): 3-13.

Roy, R.F., Decker, E.R., Blackwell, D.D., and F. Birch. 1968. Heat Flow in the United States. *J. Geophysics. Res.* 73(16): 5207-5221.

Schwartz, F.W. and H. Zhang. 2003. Fundamentals of Ground Water. *John Wiley & Sons, Inc.* New York. 583pp.

Signorelli, S. 2004. Geoscientific Investigations for the Use of Shallow Low-Enthalapy Systems. *Ph.D. Thesis, Swiss Federal Institute of Technology Zurich,* 159pp.

APPENDICIES

Appendix A

Table A.1 Multiplexer Wiring Diagram for Thermistor Cable

Port	Wire	Destination
1H	Main ground, g (black)	cable, 3H
1L	----------|--- (blue on blue)	15 ft
2H	----------|--- (blue on green)	20 ft
3H	g, g	1H, 5H
3L	| (blue on yellow)	25 ft
4H	----------|--- (blue on red)	30 ft
5H	g, g	3H, 7H
5L	| (blue on white)	35 ft
6H	----------|--- (blue on orange)	40 ft
7H	g, g	5H, 9H
7L	----------|--- (blue on purple)	45 ft
8H	----------|--- (blue on brown)	50 ft
9H	g, g	7H, 11H
9L	---------- --- (yellow on blue)	55 ft
10H	---------- --- (yellow on green)	60 ft
11H	g, g	9H, 19H (next row)
11L	(yellow on yellow)	65 ft
12H	---------- --- (yellow on red)	70 ft
RES	(green)	datalogger C2
CLK	( )	datalogger C1
G	(black), (clear)	both to datalogger G
12V	(red)	datalogger first 12V
COM Odd H	(black)	circuit board
COM Odd L	( )	circuit board
COM –o>	(orange)	datalogger -|l> btw 2L+3H
COM Even H	( )	circuit board
COM Even L	(blue)	datalogger 2H
13H	g, g	21H, 15H
13L	(yellow on white)	75 ft
14H	---------- --- (yellow on orange)	80 ft
15H	g, g	13H, 17H
15L	---------- --- (yellow on purple)	85 ft
16H	---------- --- (yellow on brown)	90 ft
17H	g, g	15H, 19H
17L	----------|--- (green on blue)	95 ft

18H	----------l--- (green on green)	100 ft
19H	g, g	17H, 11H
19L	l (green on yellow)	105 ft
20H	----------l--- (green on red)	110 ft
21H	g, g	13H, 23H
21L	l (green on white)	115 ft
22H	----------l--- (green on orange)	120 ft
23H	g, g	21H, 25H
23L	----------l--- (green on purple)	125 ft
24H	----------l--- (green on brown)	130 ft
25H	g, g	23H, 27H
25L	----------l--- (red on blue)	135 ft
26H	----------l--- (red on green)	140 ft
27H	g, g	25H, 29H
27L	l (red on yellow)	145 ft
28H	----------l--- (red on red)	150 ft
29H	g (single)	27H
29L	l (red on white)	155 ft
30H	----------l--- (red on orange)	160 ft

Table A.2 Datalogger Wiring for Thermistor Cable

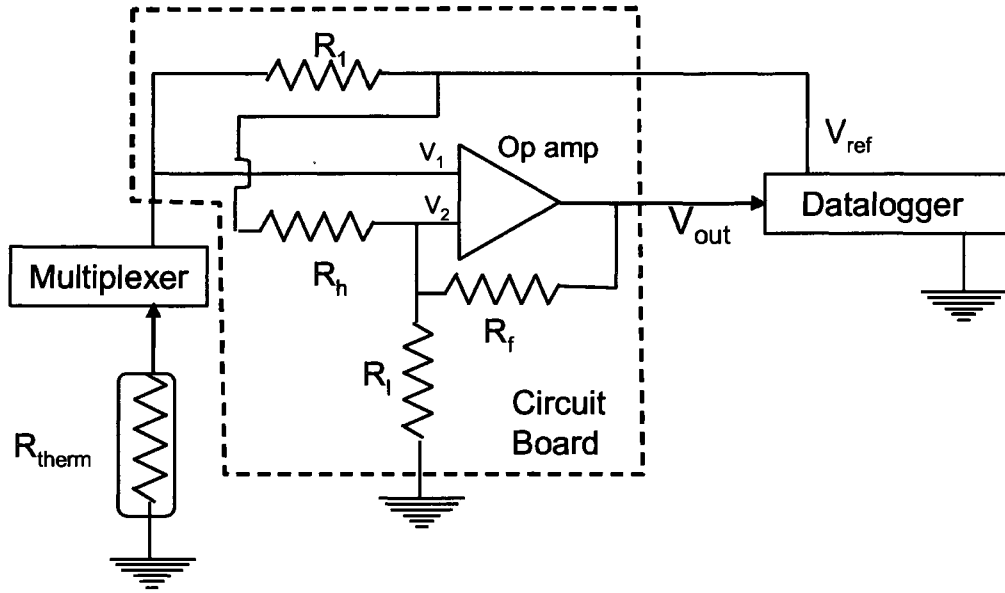| Port	Wire	Destination
1H	( )	circuit board
1L	(light green)	circuit board
-|l>	(black)	circuit board
2H	(blue)	multiplexer COM Even L
-|l>	(orange)	multiplexer COM –o>
3H (empty)	-	-
5V	(red)	circuit board
G	(black), ( )	multiplexer G (both)
12V	(red)	multiplexer 12V
C1	( )	multiplexer CLK
C2	(green)	multiplexer RES

Figure A.1 Circuit diagram for the thermistor cable, multiplexer and datalogger.

Appendix B

Table B.1 Details of heat output test of heating cable.

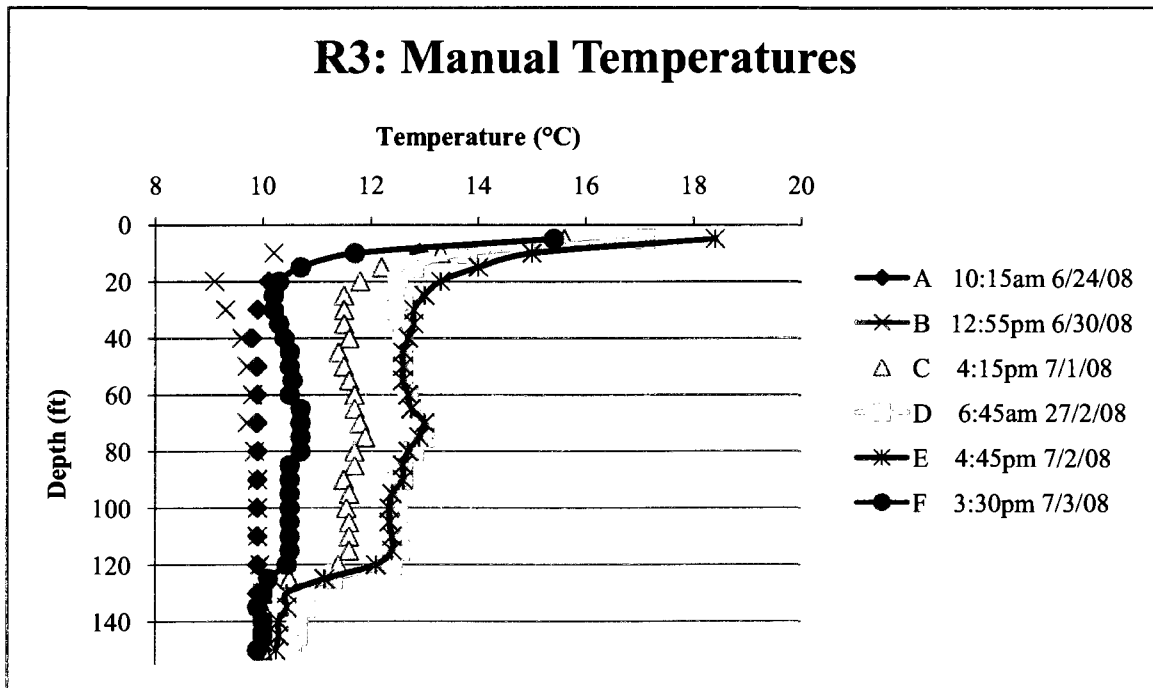| Volume of heated water	Water density (at 22.0 °C)	Mass of water	Length of submerged heating cable	Initial water temperature	Final water temperature	Change in temperature
54815 cm^3	0.9978 g/cm^3	54695 g	114.17 ft	21.8 °C	27.8 °C	6.0 °C
4.182J*54695g= 228734 Joules to heat 1°C 228734 J*6°C =1372404 Joules to heat 6 °C 1372404 J/3600 sec= 381.22 Watts 381.22Watts/114.17ft= 3.34 Watts/ft						

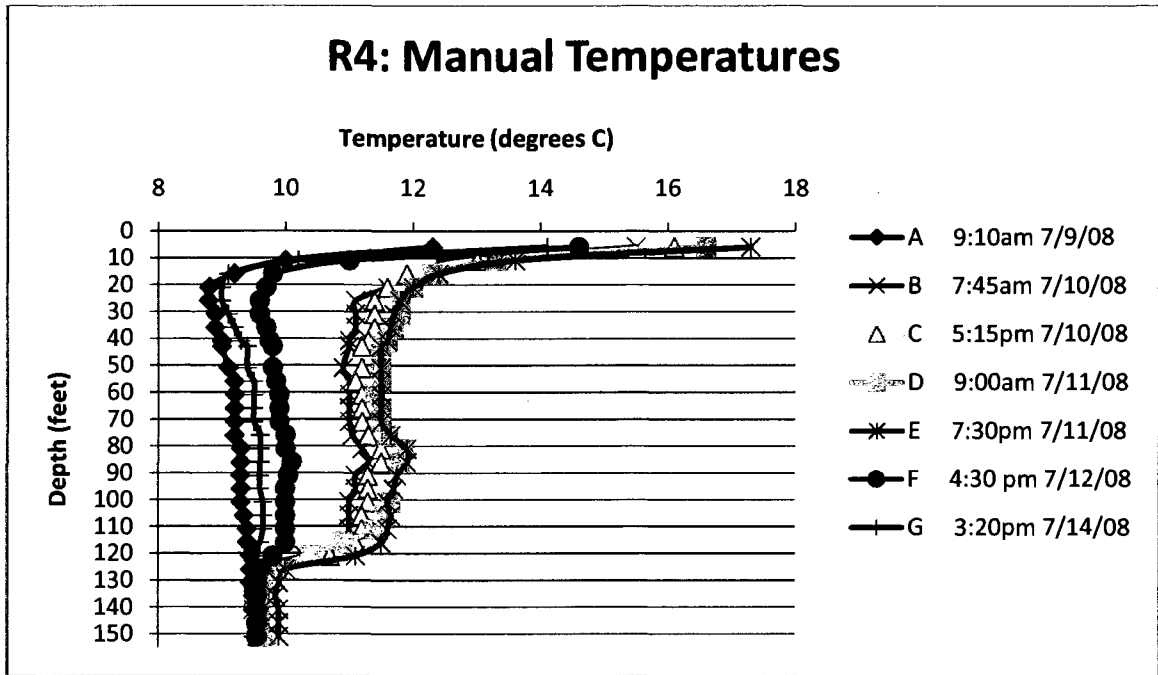**Figure B.1** Temperatures manually measured throughout heating and recovery of well R3.

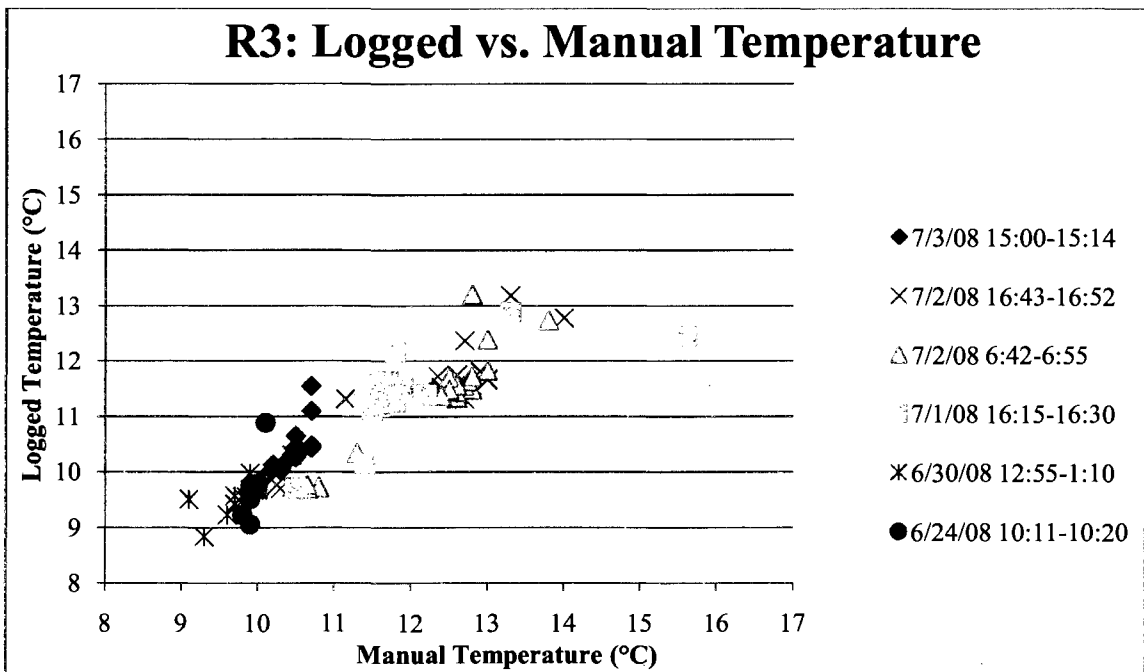**Figure B.2** Temperatures manually measured throughout heating and recovery of well R4.

Figure B.3 Temperatures logged with thermistor cable for well R3, compared to those measured manually with TLC.
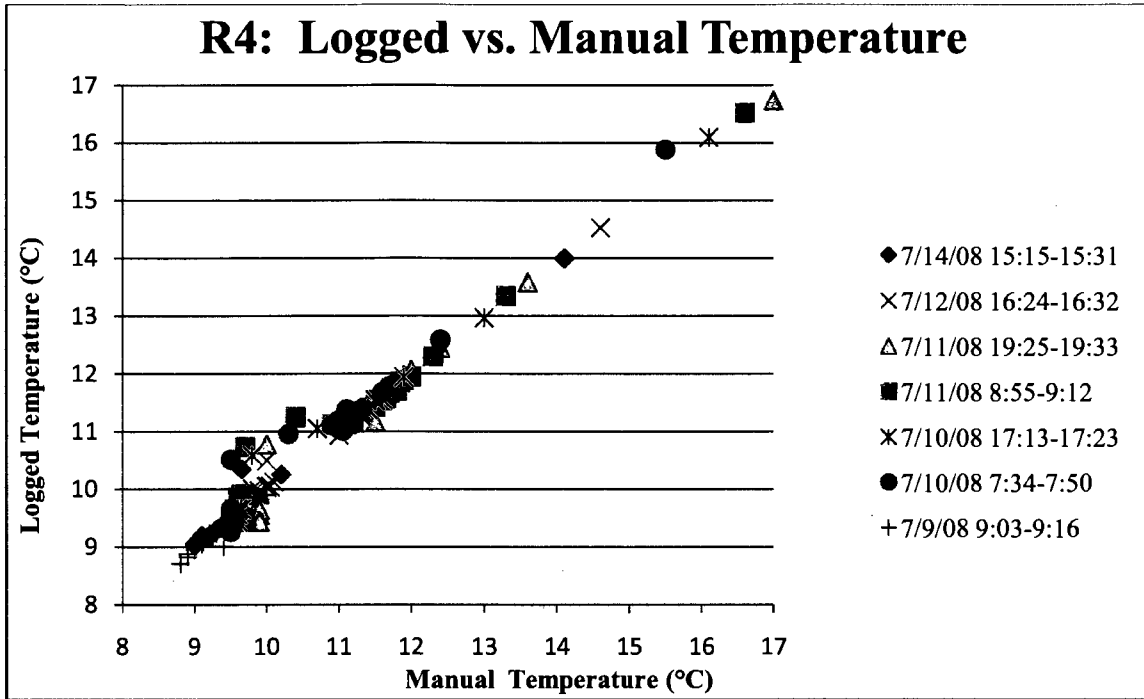
Figure B.4 Temperatures logged with thermistor cable for well R4, compared to those measured manually with TLC.
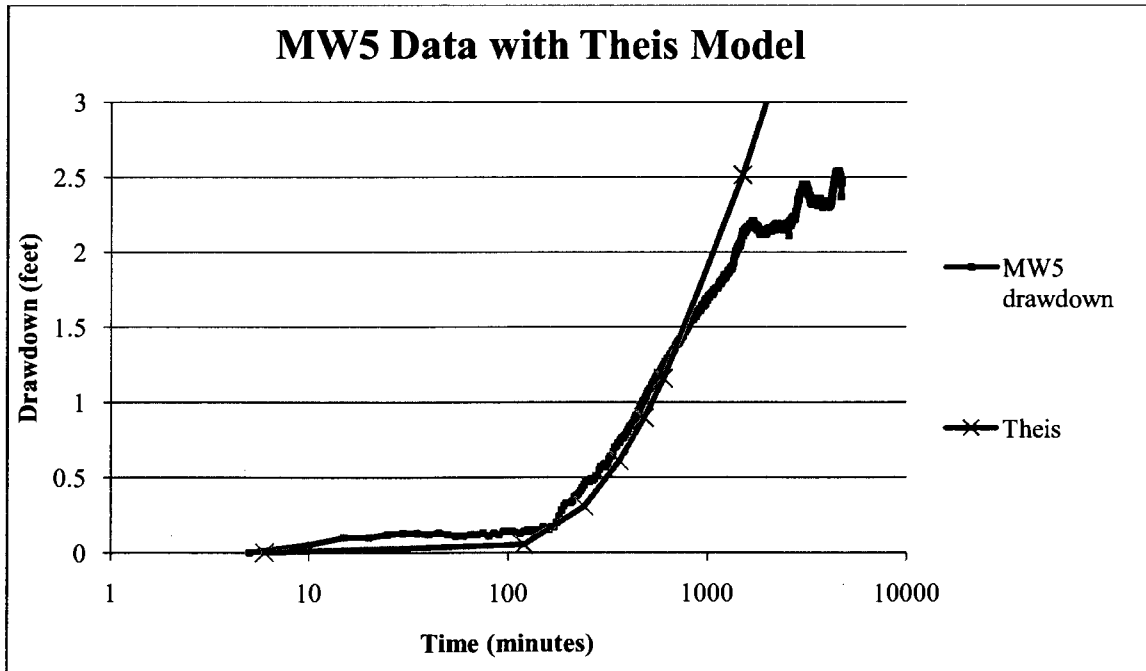

Figure B.5 Drawdown data from observation well MW5 during the pumping SR3 to R3 dipole well test. Theis curve approximates drawdown data, but has a poor fit because of the neglection of borehole storage in the Theis model. (Hydraulic conductivity 0.4856 ft/day, Sorativity 1.00×10^{-3}.)
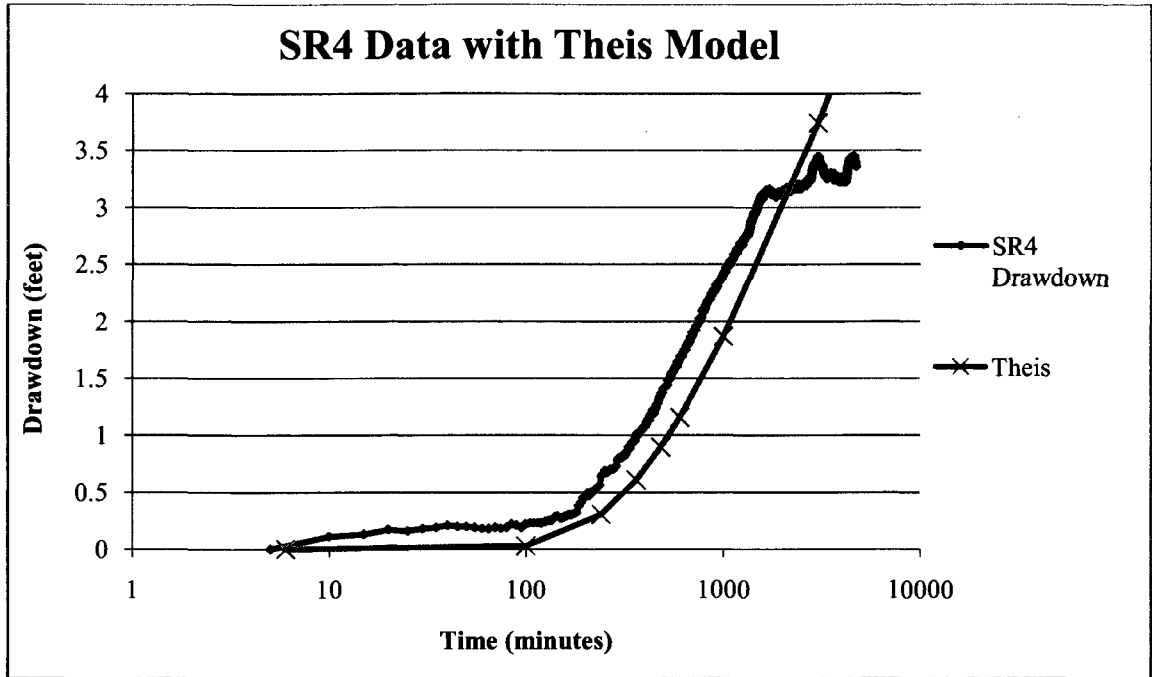
Figure B.6 Drawdown data from observation well SR4 during the pumping SR3 to R3 dipole well test. Theis curve approximates drawdown data, but has a poor fit because of the neglection of borehole storage in the Theis model. (Hydraulic conductivity 0.4856 ft/day, Sorativity 1.00×10^{-3}.)

Appendix C

Table C.1 Timeline of tests performed (listed in chronological order).

Test well	Test performed	Date	Hours
(Lab)	Calibration of thermistor cable resistivities in water tube	6/11/2008	
R2:	Background temperatures	6/18/2008	24
	Heating cable test	6/19/08-6/21/08	60
R3:	Background temperatures	06/24/2008-6/29/08	24
	Heating cable test	6/30/08-7/3/08	60
R4:	Background temperatures	7/9/2008	1.3
	Heating cable test	07/09/2008-7/11/08	60
Sr3 to R3:	Flourimeter background	8/25/2008	6
	Rhodamine tracer test Dipole well pumping	08/25/2008-8/29/08	99
R4 to R3:	Rhodamine tracer test	08/29/2008	9
	Dipole well pumping	08/29/2008-9/2/08	94
R6 to R3:	Dipole well pumping	9/2/08-9/5/08	90
	Rhodamine tracer test	9/23/2008	9